An Approach to Non-contact Respiration Monitoring in Sleeping Position Using Cameras

Submitted to
Graduate School of Information Science and Technology
Osaka University

April 2022

Prasara Jakkaew

List of Publications

Related International Journal Articles

Prasara Jakkaew, Takao Onoye, "Non-Contact Respiration Monitoring and Body Movements Detection for Sleep Using Thermal Imaging" *Sensors 20,* no.21:6307, November 2020.

Related International Conference Poster Paper

Prasara Jakkaew, Takao Onoye, "Poster: An Approach to Non-contact Monitoring of Respiratory Rate and Breathing Pattern Based on Slow-Motion Images" *2019 IEEE International Conference on Consumer Electronics - Asia (ICCE-Asia),* pp. 47-51, June 2019

Related International Presentation

Prasara Jakkaew, Takao Onoye, "Estimation of Respiratory Patterns from Video with Automatic Region of Interest Selection" *Presentation on 2020 2nd International Conference on Computer Communication and the Internet,* June 2020

Abstract

This dissertation presents an approach to non-contact respiration monitoring in sleeping positions using cameras. Firstly, the dissertation reviews existing respiratory monitoring techniques along with non-contact respiration monitoring techniques based on optical sensors and insight into a sleeping situation. In addition, the image processing technique related to the approach has been present.

Secondly, the dissertation introduces an approach to non-contact respiratory monitoring by focusing on sleeping posture using a smartphone camera-based RGB images recorded at high and frame rates. For the first challenge, the high frame rate video has been obtained and the respiratory is extracted in sleeping positions. Then, a technique is proposed with the manual region of interest selection to extract the respiratory information for estimating respiratory. For the second challenge, the ordinary video was used in the sleeping position with changing background views where subjects are covered with a black blanket. This approach presented the automatic region of interest selection technique and was compared with whole frame and human body area detection. The results show that the body's boundary as shoulder, chest, and abdominal is mainly related to the breathing movement in the sleeping position. Moreover, the ROI selection is found as a significant issue in vision-based respiratory estimation.

Thirdly, the dissertation adopts an approach to monitoring the respiratory in an actual sleeping situation using a thermal camera plugged into a smartphone. Moreover, body movement during sleep has been investigated in this study. The automatic ROI selection can be used to acquire the respiration signal and detect body movements. The results show that the respiratory rate was successfully estimated with an RMSE of 1.82 ± 0.75bpm. Next, the adoption of technology acceptance of the user's perspective has been evaluated using effort expectancy questions based on the UTAUT model. The result shows that the participants were satisfied to use a thermal camera to monitor respiratory while sleeping at home.

The dissertation emphasizes the significance of using cameras to monitor the respiratory during sleep. The ROI selection in sleeping posture was proposed to capture the respiratory information and also body movements. The proposed approach deals with the challenges of uncontrol scenarios during sleeping that has difficulty in selecting the ROI. Achievements of this dissertation would be a guideline for the further development of technology in healthcare.

Contents

List of Figures

List of Tables

Chapter 1
Introduction

This chapter describes the background and objectives of this thesis focuses on developing a non-contact respiration monitoring system to monitor respiration and body movements during sleep to be applied in a real environment. The respiratory system and irregular respiratory during sleeping are discussed. Existing respiratory monitoring techniques are reviewed and non-contact respiration monitoring techniques based on computer vision are also presented. Finally, the objectives and contributions of this thesis are explained.

1.1 Background

Respiration is a significant predictor of serious illness. The early detection of abnormal respiration can reduce the risk of acute respiratory disorders and lower associated morbidity and mortality. A respiratory rate should be tracked throughout sleep periods because over half of all patients, who suffer a severe adverse event in the general wards (such as a cardiac arrest or ICU admission), had a respiratory rate higher than 24 bpm [1]. An increase in respiratory rate is found until 24 hours before the severe event with high specificity. Approximately 50% of patients with heart failure have sleep apnea, and 20% of heart-failure related deaths occur at night [2]. Besides, several studies were shown that an abnormal respiratory rate (RR) is a predictor of such cardiopulmonary arrest [3], [4], chronic heart failure [5], pneumonia [6], pulmonary embolism [7] [8], weaning failure [9], and overdose [10]. The current gold standard for sleep monitoring and assessment is performing overnight polysomnography (PSG) at a sleep clinic that uses many sensors to measure vital signs during sleep in various settings. The PSG consists of a

simultaneous recording of multiple physiologic parameters related to sleep and wakefulness. The physiologic parameters such as brainwaves, eye movements, heart rate, breathing pattern, blood oxygen level, body position, chest/abdominal movement, limb movement, and snoring are recorded by multiple sensors attached to the patient's body. The PSG was performed overnight and was continuously monitored by a credentialed technologist. However, this process is an expensive, time-consuming, and labor-intensive, and the test subject has a cramped feeling while asleep.

Nowadays, the technology for monitoring respiration is growing rapidly. Various studies perform non-contact respiratory monitoring during sleep with different techniques. The Wi-Fi-based techniques are used to track people's vital signs by exploiting channel state information extracted from the Wi-Fi physical layer to detect the minor motions caused by breathing and heartbeat. A Doppler radar is also used to capture the subject's movement and breathing signal. The limitation of such techniques is related to the high cost of instrumentation, the need for specialized operators, and a low signal-to-noise ratio, making them impractical for large-scale deployment. Some approaches have been investigated to monitor the respiratory in a different situations, like a pressure-based method. Most non-contact techniques used to monitor respiratory are based on optical sensors because it is a growing preeminence owing to the recent progress in video technology. Both simple cameras and specialized cameras have been used to measure and monitor respiration like a webcam, depth, infrared, and thermal cameras [11]-[16].

The precision of detected breathing area while a user is sleeping plays a vital role in monitoring daily life. Many researchers have analyzed video and image sequences to detect the motions and extract a vital sign in a sleeping position. For example, in the works of Nakajima et al. [17] and Frigola et al. [18], the breath rate is computed by measuring the chest movement by analyzing the optical flow vectors. Kaiyin Zhu et al. [19] proposes a tracking algorithm of the upper torso's motion and head using an infrared camera during unconstrained nocturnal sleep. Sato and Nakajima [20] calculate the volume change amount using fiber-grating 3D vision sensors to monitor the bright spots moved by inhalation. Ching-Wei Wang investigated sleep apnea using infrared video [21]–[25]. Ali Al-Naji [26] proposed a motion magnification technique to magnify the baby's respiratory chest movements. Their studies demonstrated that the respiratory rate could be assessed successfully using a Digital Single Lens Reflex (DSLR) camera shooting the baby's chest at different positions, even in the presence of a blanket on the baby or unclear region of interest (ROI). Ilde Lorato [27] presented a camera-based online short

cessation of breathing using a CCD camera. Although various studies adopting video cameras are used to monitor the respiratory system during sleep, there are no results regarding the validity of such methods in practice since most of these studies offer the experiment testing by controlling the environment or under the sleep simulation [28]-[30]. The respiratory monitoring should be performed continuously, and it is reasonable to monitor that RR using simple electronic devices. However, the main challenge commonly emphasized is the limited use of respiratory systems to screen and monitor everyday life in a variety of sleep environments where noises are associated with the unpredictability of body movements, body orientations, and changes in the environment sleeping posture.

Therefore, this thesis focuses on a non-contact respiratory measurement in the sleeping position using an accessibility device and easy to use with a smartphone. This study considers the various bedroom environments with different conditions like a room background, lighting, bed, blanket, and pillow. Then our approach should be able to provide accurate respiratory monitoring under such challenging conditions. The target group of this study is people who live alone and have a symptom of irregular breathing because they are unaware of their symptoms without being reminded by their partners. They require screening before going to a hospital for taking a sleep test. The benefit of screening for respiration problems is monitoring breath activity continuously under natural physiological conditions in a sleep environment, reducing the cost of a complete sleep test, and reducing the risk of serious illness associated with respiration.

1.2 The Role of Respiratory

The respiratory system is the gas exchange process to take in oxygen and expel carbon dioxide as breathing moves air in and out of the lungs. The structures involved in the breathing process consist of the nose, airways, and lungs. This inspiratory and expiratory process occurs with the thorax and abdomen's synchronous movement. The frequency of breaths over a period of time is defined as a respiratory rate usually measured by counting the number of breaths a person takes per minute. Therefore, the clinical staff can count the number of times the chest moves up and down for a full minute. The typical respiratory rate for healthy individuals is 12–20 breaths per minute [31]. Like a bit of change, three to five breaths per minute have a critical predictor of serious illness with changes in the patient's condition. A rate of less than eight bpm or a decreasing RR may also signify deterioration. Besides, shortness of breath at rest is a sign

of a medical problem. Various abnormalities cause shortness of breath in different organ systems in the body (lung, heart, systemic illness, nervous system) [32]. Goldhill and colleagues' study reported that a patient with a 25–29 bpm respiratory rate had a 15-25% hospital mortality rate [33].

Therefore, the early detection of abnormal respiration can reduce the risk of acute respiratory disorders and lower associated morbidity and mortality. Although the respiratory rate indicates a clinically severe event, respiratory rate measurement is still widely performed by manual counting, making inaccurate results [34] or neglected [35]. Respiratory rate was often not documented routinely, actually when the patient's primary problem is a respiratory condition.

1.3 Respiratory Monitoring Techniques

The respiratory rate could be recorded with various techniques in the clinical, including contact and non-contact methods. The breath measuring approaches can derive breathing parameters from body surface motion detection by inferring thoracic volume changes. A continuous breathing monitoring system uses either wearable (respiratory inductance plethysmography, resistance-based sensors, capacitance-based sensors, inertial measurement units, fiber optic sensors) or non-wearable devices (mechanical ventilators, long-term oxygen therapy, polysomnography). Some wearable devices require cumbersome and expensive apparatus that may interfere with natural breathing and can be unmanageable in specific applications such as ambulatory monitoring, stress testing, and sleep studies. For example, Respiratory Inductance Plethysmography (RIP) uses two transducer bands placed around the subject to measure the chest and abdomen movement. Several wearable sensors are based on the principle that the measured resistance varies with the torso's movement. An example is the Go Direct Respiration Belt, which uses a force sensor and an adjustable nylon strap around the chest to measure respiration effort and respiration rate.

Non-wearable devices are used in continuous monitoring of breathing performed with unobtrusive devices as Long-term Oxygen Therapy (LOT). There are commercial devices to calculate the RR via a sensor that detects pressure changes in the oxygen line. Nowadays, sleep respiratory monitoring comprises different measuring methods with specific sensors or measurement techniques that depend on applications, environments, limitations, requirements, and user needs. There are various approaches for respiration monitoring, categorized into contact and non-contact respiratory monitoring methods described in the following section.

1.3.1 Contact-based Respiratory Monitoring

In contact-based measuring methods, various sensors (i.e., airflow sensors, acoustic sensors, carbon dioxide sensors, strain sensors, movement sensors, bio-potential sensors, temperature sensors, and humidity sensors) are attached to the subject's body. The sensors must be positioned in a different body area to detect respiratory sounds, respiratory airflow, respiratory-related chest or abdominal movements, air temperature, air humidity, and respiratory CO_2 emission [36], as shown in Table 1.1.

Table 0.1 Contact-based Respiratory Monitoring Techniques.

Techniques	Measurements	Sensors/Devices	Body area
Respiratory sound	Acoustic	Microphones	Nose, Mouth, Neck, Chest
Respiratory airflow	Flow	Differential flowmeters (mechanical ventilators, spirometers), Turbine flowmeters (spirometers, metabolic cart), Hot wire anemometers, Fiber optic sensors	Nose, Mouth
Respiratory-related chest or abdominal movement	Strain	Resistive sensors, Capacitive sensors, Inductive sensors, Fiber optic sensors	Chest, Abdomen
	Impedance	Transthoracic impedance sensors	
	Movement	Accelerometers, Gyroscopes, Magnetometers	
Air temperature	Temperature	Thermistors, Thermocouples, pyroelectric sensors, Fiber optic sensors,	Nose, Mouth
Air humidity	Relative humidity	Capacitive sensors, Resistive sensors, Nanocrystal and nanoparticles sensors, Fiber optic sensors	Nose, Mouth
Respiratory CO_2 emission	CO_2	Infrared sensor, Fiber optic sensors	Nose, Mouth
Cardiopulmonary	Electrophysiological signal	ECG sensors	Heart muscle
	Light intensity	PPG sensors	

1.3.2 Non-Contact based Respiratory Monitoring

Non-contact respiratory monitoring methods are usually based on radar, Wi-Fi, thermal, and depth image sensors, which do not involve anybody's surface contact. These have been done using different techniques, including those based on thermal imaging [37], depth imaging [38], infrared imaging [39], and RGB imaging [40]. Several techniques are categorized based on measurement, where Massaroni et al. [41] identified four different classes, including techniques based on environmental respiratory sounds, air temperature, chest wall movements, and cardiac activity modulation, as shown in Table 1.2. The respiratory sound approach is often used to detect apnea and snoring events. In some scenarios, the respiratory estimation from sounds is difficult to retrieve robust respiratory sounds because of the intrinsic susceptibility of breathing sounds to various environment interferences. The Wi-Fi [42] and radar [43] approaches can measure respiration based on radio frequency through wireless electromagnetic signals in 3kHz-300GHz. In [44], researchers used a Wi-Fi signal to monitor breathing and heart rate for different sleep postures in real-time. Another work [42] used a Wi-Fi network to capture the movements caused by breathing and heartbeats during sleep in a realistic setting (bedrooms). The Wi-Fi-based approaches were evaluated only during short-duration sleep experiments in very controlled settings, which would be a limitation in the natural environment with breathing-unrelated movements.

Table 0.2 Non-Contact based Respiratory Monitoring Techniques.

Techniques	Measurements	Sensors/Devices	Related area of the body
Respiratory sound	Acoustic	Microphones	-
Air temperature	Temperature	Thermal cameras	Nose, Mouth
Chest wall movement	Body movement	Depth sensors	Neck, Top body
		Radar sensors	
		Wi-Fi sensors	
		RGB cameras and visible light sensors	
Cardiac activity modulation	Light intensity	RGB cameras	Face, Neck, Shoulder

Non-Contact Respiration Monitoring During Sleep

Respiration and statistics of sleep events are essential indicators of sleep quality, stress level, and various health conditions. Traditional approaches use many sensors to measure vital signs during sleep in various settings environment. Such systems incur high costs and are usually limited to clinical usage. Especially as mentioned before, the non-contact method is appropriate for automatic, reliable, and convenient sensors and devices to monitor the respiratory rate during sleep. It should be performed continuously for a long time without impressing the patient's burden. Various studies perform non-contact respiratory monitoring during sleep with different techniques, as shown in Table 1.3. Works in [42] [44] collect the wireless channel state information (CSI) of the radio signals and extract rhythmic patterns associated with breathing and abrupt changes due to body movement. However, CSI cannot identify getting-ups or hand movements activities, and thus it is very hard to track a person's respiration in the presence of these activities. In addition, the minimum transmission power should be set without decreasing the system's performance for tracking a person's sleep even for different persons and in different room environments. Doppler radar is also used to monitor vital human signs [43] [45]. It relies on the modulation effect due to the chest-wall displacement of a radio signal towards the patient. However, several other factors should also be measured close to or within the device, such as room temperature, sound, and light exposure. Moreover, complex signal processing techniques are required to detect and measure these vital signs accurately, and these techniques significantly increase power consumption.

In general, the respiration information is captured by a video camera containing helpful information about respiration activity. Many researchers have analyzed video and image sequences to detect the motions and extract vital signs in a sleeping position. Several approaches investigated to monitor the respiratory through infrared, thermal, and depth video [11-14], [38], [46–52]. Simple commercial cameras are low-cost and easy to use for measuring physiological signals. However, a specialized camera like a thermal camera is suitable for sleep monitoring because it can classify the human from the background even when turning off the light. There still exist challenging issues that the achievements on non-contact physiological vital signs estimations are generally based on “stationary” and “direct-facing” subject measurements, which is not ideal for sleep monitoring.

Table 0.3 Summary of non-contact respiration monitoring during sleep.

Techniques/ devices	Authors	Year	Proposed	Measurement	Performance	Limitation	Challenging
Wi-Fi based method	Jian Liu [42]	2018	Monitor respiratory rate, heart rate, and posture	CSI	RR: more than80% estimation errors are less than 0.5 b/min, HR: 57% of estimation errors are less than 2 b/min and over 90% of estimation errors are less than 4 b/min, Posture identification: > 90%	The experiment was simulated in each sleep postures.	It should be performed in an actual sleep situation.
	Yu Gu [44]	2019	Breathing and heart rate	CSI	MAE: 0.575 bpm for detecting breath, 3.9 bpm for detecting heart rate. The overall accuracy is 96.636% and 94.215%.	The experiment was performed in a short time.	It should be performed in an actual sleep situation.
Doppler radar-based sensor	Feng Lin et al. [43]	2017	Recognize sleep status (on-bed movement, bed exit, and breathing section)	Sleep status recognition framework	Accuracy: 95.1% (Short term-controlled environment) Error: 6.65% (75 min in real life)	The experiment was simulated in each sleep postures in short term.	It should be performed in an actual sleep situation.
	Mari Z [45]	2015	Respiration	Using a center estimation method and the arctangent channel combining method	The coverage of successfully demodulated radar data was ~58%–78%.	The length of the epochs used for center estimation in this study was probably not optimal.	The epoch lengths should be automatic setting.
Infrared vision-based methods	Geertsema E [46]	2019	Detect central apnea	The arrest of oscillatory breathing	Specificity: 99%	False detections in which a very small movement precedes a larger movement	Classify movement is required
	Kaiyin Zhu et al. [47]	2019	Respiratory and heart rates	Motion analysis by using PCA and	Accuracy: 89.89% for BR, 77.97% for HR	Unable to isolate respiratory and heart	Classify movement is required

Techniques/ devices	Authors	Year	Proposed	Measurement	Performance	Limitation	Challenging
				ICA	RMSE: 2.10 bpm, 7.47 bpm	beat during periods with large movements	
	Fei Deng [48]	2018	Breathing, head posture, and body posture	Motion magnification	Accuracy: 96% in recognizing abnormal breathing and body movements, 87.6% in head tracking, and over 90% in classifying most body postures.	Use simulation data set that the thresholds of the algorithm may have to be changed when applied in an actual situation	It should be performed in an actual sleep situation.
	Michael H Li et al. [49]	2017	Respiratory and heart rates in different sleeping position	Identify and track feature point (chest motion)	Error: 3.4% for BR, 5.0% for HR	Motion tracking with optical flow may suffer if regions lack texture when white sheet offers enough texture.	Automatic sleep position identification and handle unwanted motions.
	Michael H Li et al. [50]	2014	Respiratory rate	Feature point analysis and PCA	Accuracy: 97%	Small sample size (five participants) in simulate overnight sleep	It should be performed in an actual sleep situation.
	Abbas K Abbas [51]	2011	Monitor respiratory of neonatal	Temperature change in the nostril's region	N/A	A variation in background temperatures, the neonate's respiration was manually registered	Automatic ROI selection
Video based method (Thermal)	Usman [52]	2019	Respiratory	Temperature fluctuations	70% well corelated	The subject did not have large body movement and the camera is fixed, the face may not remain within the camera's field of view	Detect the reparation without face detection

Techniques/ devices	Authors	Year	Proposed	Measurement	Performance	Limitation	Challenging
Video-based method (Depth sensing + invisible near infrared illuminator)	Bernal E [38]	2014	Respiratory	Respiratory motion of the chest and abdomen	N/A	Accuracy of measurements on subjects wearing loose clothes that occlude the visibility of the respiratory motion of the chest and abdomen can be a drawback.	Detect the reparation with various clothes
Video based-method (RGB)	Cobos-Torres J [12]	2018	Monitor respiratory, and heart rate of neonatal	Analysis the color intensity variations	Correlation coefficient: 0.86 for BR, 0.94 for HR	It would not work in the case of poor lighting or darkness.	It could be improved to detect in a dark environment
	Mauricio Villarroel [13]	2017	Respiratory rate, heart rate, and detect change in peripheral oxygen saturation in the clinic	Face detection and tracking algorithm	MAE: 2.1 bpm for over 69% of the time for BR, 2.8 beats per minute for over 65% of the time for HR	The experiment was carried out in similar condition as patients' upper torso at a similar distance from the camera.	It could be improved to detect in a dark environment and various conditions
	L Tarassenko [14]	2014	Respiratory rate, heart rate, and oxygen saturation change	Ambient light and auto regressive models	N/A	It would not work in the case of poor lighting or darkness.	It could be improved to detect in a dark environment and various conditions
Video based-method (Depth)	Matsuura Y [11]	2017	Screening sleep disorder	Moving average	N/A	The bodies movement or posture change temporarily affected the monitoring of the respiration condition	Classify movement is required
Pressure-based method	Lorcan Walsh [53]	2014	Monitor respiratory and sleep events	The amount of light passing between an emitter and receiver woven into a semi-	Mean difference of 0.12 breaths per five minutes and a mean percentage error (MPE) of 0.16%	N/A	N/A

Techniques/ devices	Authors	Year	Proposed	Measurement	Performance	Limitation	Challenging
				permeable substrate			
Impulse-radio ultra-wideband radar (IR-UWB Radar)	Sun Kang [16]	2020	Sleep apnea	Respiratory events	Intraclass correlation coefficient = 0.927). The overall agreements of the impulse-radio ultra-wideband radar were 0.93 for Model 1 (AHI ≥ 5), 0.91 for Model 2 (AHI ≥ 15), and 1 for Model 3 (AHI ≥ 3	A fixed distance between the radar and subject.	It required in various setting environments.

The challenge of optical sensors-based methods that have been investigated in many studies is the accuracy of respiratory detection. The advantage of camera-based methods is an attractive sensing option that offers comfort in measuring the patient's respiration. The respiratory is related to movements of the abdominal area, face area, area at the edge of the shoulder, and a pit of the neck. The video extracts the respiratory signal based on image subtraction, optical flow analysis, Eulerian Video Magnification (EVM), and Independent Component Analysis (ICA) applied to pixel intensity changes.

By the review of literature works, several approaches have been proposed to select an ROI related to breathing movement to estimate the respiratory rate using a smartphone camera. In 2001, Nakajima et al. [54] reported that small areas or ROI could be detected in real-time without a high-speed image processor, although the ROI would have to track the subject's movement. Takemura et al. [55] introduced a technique to extract a partial region with a respiratory movement as the ROI by creating several small partial areas in the same area and then evaluating their up and down motion. Wiesner and Yaniv [56] presented a respiratory monitoring system using a single optical camera that tracks the motion of color fiducials placed on the abdomen. Zhao et al. [57] identified ROI by detecting the face and upper body positions of the subject and then selecting the area between the bottom of the face region and the upper body region with a width equal to 80% of the width of the upper body region as the ROI for respiratory measurement. Bartula et al. [28] obtained the ROI through a projection like a transformation onto a vertical axis. The region is selected from the most influential motion component of natural person camera geometry along that axis. Tarassenko et al. [14] identified an ROI within the subject’s face. The size of an ROI for respiratory rate estimation is usually smaller than that for heart rate estimation. This study recommended that a small area, e.g. ROI, could be more suitable for respiratory evaluation. Li et al. [50] presented a respiratory rate estimation method in which each frame is divided into 10 × 13 grids, and then feature points are extracted from each grid. Makkapati and Rambhatla [58] projects a circular dot of light onto the chest and abdomen region of the subject and observes the change in the shape and size of the spot so as to derive the respiration signal at a given frame. Lin et al. [59] locates the face and upper body area and detects the salient ROI by Haar-like features with their responses converged by interquartile range. Wei et al. [60] measured the respiratory rate by selecting a dual ROI on a facial video image. Wiede et al. [61] selected the ROI from face detection and upper body detection, which are available in the sitting position. Other researchers have monitored the respiratory rate at the neck's pit rather than from the chest or abdomen [62]. An

ROI is determined by selecting the pixels at the pit of the neck that is the anatomical point near the suprasternal notch. The dip between the neck and the two collarbones is significant and visible enough to be easily identified. Shao et al. [63] selected a region of 40 × 40 pixels around the edge of the shoulder for breathing detection. The size was large enough to capture the complete range of possible shoulder movement due to breathing activity. Cobos-Torres et al. [12] measure a newborn's two vital signs by calculating the intensity of pixels with 40×40 pixels.

Most studies select regions of interest based on breath movement (e.g., from the face, chest, torsos, abdomen, shoulder, or pit of the neck), which can be identified when the subject is sitting in front of a camera. However, in a practical situation, the face and torsos are not completely visible in sleeping, and body and skin pixel detection is usually disturbed by blankets. Therefore, it is more challenging when the subject is in a sleeping posture. The Eulerian video magnification method features estimation in a sleeping position where whole frame imaging is executed to amplify a small motion such as blood flow or respiratory movement that can hardly be seen with the naked eye [64]. In Naji and Chahl [26], the chest area was selected as the ROI, and breathing movement inside the ROI is magnified by using wavelet decomposition and an elliptic filter. This ROI-based method resulted in fewer errors than that of the Eulerian video magnification method, which was accompanied by noise and artifacts.

It is known that the size of the region may affect respiratory monitoring accuracy. The ROI selection is the primary key when extracting the respiratory signals from video images, and one of the significant challenges is to enable automatic ROI selection while sleeping to detect small movements that occur during breaths. Typically, the respiration signal incurs large distortion when the subject moves, and the accuracy is degraded [65]. A few studies treat automatic ROI selection for respiratory monitoring. In 2013, [57] detected the face and upper body to locate an ROI in a similar manner with [40][59] for motion analysis by using a signal-to-noise ratio (SNR) in estimating the temporal properties of a velocity waveform. Janssen et al. [66] presented an automatic ROI selection, which can reject the non-respiratory motion. In 2018, [67] proposed an automatic selection of ROI through means of the extracted periodic features presented in [68].

The above study detects respiration information using a simple camera to obtain the video in a sitting position with visible light. The ROI selection was performed to limit the observed area, increasing the accuracy of respiratory estimation. Thus, any method needs to pay attention to

selecting the body related to the breathing area in the sleeping position. One of the experiments in this thesis uses a smartphone to obtain the video and presents an automatic ROI selection for accurate breathing area.

1.4 Research Contributions

Based on the above survey of literature works, the objectives and the contributions of this research are described here. This research aims to propose an approach to monitoring respiration in an actual sleeping situation using an accessibility device in various conditions.
First, we discover the suitable ROI location and size when using an optical sensor to monitor respiration in a sleeping position. The proposed method focuses on automatically selecting the size and location of the ROI to improve the accuracy of respiratory estimation in sleeping posture. Limiting the observed area in an image frame can reduce the processing time, and make respiration monitoring more accurate. Besides, motion detection has been employed to locate the breath movement area. In this research, edge detection has been used to detect the body's boundary when the subject lies down on the bed. This stage of the simulation experiment has a limitation of the background pattern and cloth pattern that disrupt the edge detection. Secondly, non-contact respiration monitoring for an actual sleep environment using the thermal camera is proposed. Several test scenarios were carried out with various bed covers or blankets in dim light and uncontrolled sleeping positions to test the reliability. The body movements are also analyzed. Finally, user acceptance has measured the level of ease of use associated with the use of new technology.

1.5 Thesis Outline

Chapter 2 introduces a non-contact respiration monitoring technique based on a simple camera and a solution for estimating respiration from the sleeping posture. A smartphone camera is used to record an RGB video at a high frame rate and an ordinary frame rate. We focus on the respiratory ROI selection, especially in sleeping posture. An uncontrollable sleep posture makes it challenging to find an area to detect breathing movements significantly related to respiratory measuring accuracy. Different from the sitting posture that can be easier seen on camera in a sitting position and monitoring breathing from a conscious person. Then Chapter 3 proposes a non-contact respiration monitoring technique for an actual sleep environment

using thermal imaging in a dim environment. Experiments are carried out in an actual sleeping situation in the participant's bedroom. Chapter 4 presents the user acceptance-based effort expectancy of users after they try to use this preliminary system to record their sleeping by themselves. User acceptance of health monitoring is studied to understand the factors that affect the intended users' perception. Finally, concluding remarks and future work are given in Chapter 5. The thesis outline is shown in Figure 1.1.

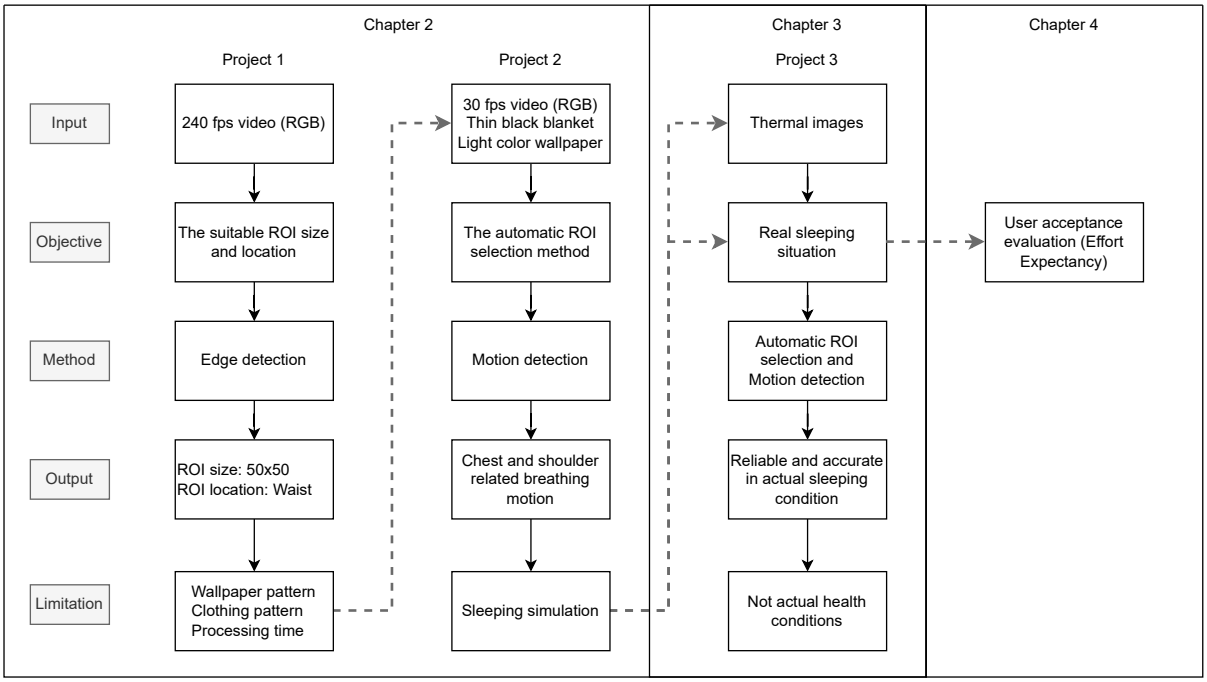

Figure 0-1: Outline of the thesis.

Chapter 2
Non-Contact Respiration Monitoring in Sleeping Position using Smartphone Cameras

This chapter discusses non-contact respiratory monitoring in sleeping posture via smartphone camera-based RGB images. Experimental tests of extracting respiratory values with high frame rate video (240 fps) and ordinary video were executed by smartphone with the objects lying down on the bed.

2.1 Introduction

As discussed in Sect. 1.1, non-contact respiration monitoring based on camera imaging has comfort for the patient and accessibility. Due to this, a patient who has a smartphone can utilize this method for monitoring themselves at their home. The respiratory in sitting position has been proposed in literatures, but only a few works focused on sleeping positions. The non-contact respiratory monitoring in sleeping posture via smartphone camera-based RGB images with different frame rates is investigated in this study. The higher than 30 fps in terms of the frame rate is used to create a slow-motion video to ensure a higher level of detailed information for the motion capture. This study also records 240 fps because the respiratory is a very tiny motion, and more frames may provide details, allowing for more flexibility. The movement

during sleeping is referred to the breathing (inhalation and exhalation). Inhalation (also known as inspiration) happens when air or other gases enter the lung. Exhalation (or expiration) is the flow of the breath out of an organism. In humans, air moves from the lungs out of the airways to the external environment during breathing. Respiratory-related body movement can be monitored by using optical sensors. Typically, an area at the edge of the shoulder [69], the pit of the neck [70], the thorax[22][59][67], the thoracoabdominal area [71], and the abdomen movements could be used to measure respiratory rate values by using a built-in notebook camera [72], built-in smartphone camera [73], and CCD camera [22]. Then, the video is recorded to retrieve respiratory patterns from video frames.

Different approaches have been used to postprocess the pixel data to extract signals related to the respiration from such videos by the subtraction of two continuous images [6, 9], analysis of pixel intensity changes based upon independent component analysis [10, 74], analysis of average contributions of red, green, and blue channels of the video [75, 35, 36], analysis of optical flow [7], and magnified the movement.

In the pixel intensity change based approaches, the breathing pattern can be determined by detecting and analyzing body movements associated with breathing. For example, Yunyoung Nam et al. estimated the respiratory rate from the chest and abdominal motions using the front-facing video camera [76]. They found that the use of the maximum peaks based on the Welch periodogram provided an accurate breathing rate for low and high breathing ranges (0.1–1 Hz). However, this approach did not always provide satisfactory results at the medium to high breathing rates (0.4 and 0.5 Hz), especially when subjects wore either loose clothing or breathed shallowly. Massaroni et al. extracted the respiratory pattern from intensity variations of reflected light at the level of the collar bones and above the sternum [70]. The influence of the video sensor resolutions, i.e., HD 720, PAL, WVGA, VGA, SVGA, and NTSC, have been evaluated. In their experiments, the HD 720 resolution indicated perfect agreement with average breathing frequency values gathered by the proposed measuring and reference instruments. The video recorded at a set frame rate of 30 Hz is enough to discretize the breathing movements that generally happen up to 60 breaths per minute, equal to 1 Hz. This method collects the respiratory pattern from the chest wall motion by selecting an ROI, and analyzes the intensity change to extract the breath-by-breath respiratory rate.

Although several studies acquired video data with different frame rates at 4-30 fps [28][12], [22], none tried high frame rate video capturing more images in a second for smooth video. Besides, many studies were developed for adult subjects sitting in front of the camera, for

which it is easy to select the ROI and analyze the respiratory because the pit of the neck is large and easily identifiable.

Then, respiratory monitoring in sleeping positions has been studied for newborns with manually cropped images that contain only the chest and abdomen region [29]. Alinovi et al. [67] used the Maximum Likelihood (ML) approach to perform ROI selection, ML data fusion, and RR estimation. The selected area is still near the chest of the newborn patient. This study confirms that the chest area is strongly related to breathing movement in lie-down posture. However, the ROI size also affects respiratory estimation. In addition, environmental conditions have a strong influence on image signals, for example, the noise from light, the distance between subjects and camera, clothing, and background view [61]. The distance from the camera to a subject is generally set between 0.5 meters to 3 meters. Shao et al. set the distance at 0.5 meters, and Massaroni et al. set the distance at 1.5 meters for the first study and then at 1.2 meters in the second study. Wiede et al. [61] considered the distance from the camera, the brightness of the image, the influence of different clothing, and the back view. They recommended using FFT and Welch methods to determine the frequency of the respiratory signal. In the experiment, the distance (1 meter, 3 meters), the illumination, and the influence of clothing did not substantially affect the algorithm. However, the slim-fit T-shirt was provided for better performance than the loose-fit T-shirt [62]. So, the clothing and background view should be considered when taking the experiments. Besides, the camera distance is not significant for the accuracy of respiratory estimation, but it depends on whether the subjects are available in the camera view.

Therefore, despite the large number of studies adopting video cameras for respiratory monitoring purposes, there is a lack of results about the validity and accuracy of such methods in practice since most of these studies present proof of concepts or preliminary tests. This chapter presents non-contact respiratory monitoring in sleeping positions based on the RGB images recorded by a smartphone camera. The aim of the present study is three-fold: (i) an approach of non-contact monitoring of respiration in sleeping positions by using RGB video signal acquired from a built-in smartphone camera; (ii) the experimental test of this monitoring approach in extracting the respiration values from high frame rate video and ordinary video; and (iii) the evaluation of the accuracy of ROI selection and ROI size for sleeping position.

2.2 High Frame Rate Video Experiment

2.2.1 Proposed Method

Assuming that the high frame rate video contains greater details, this experiment proposes a respiratory rate and breathing pattern estimation method shown in Figure 2.1. The first step of the processing is to record the RGB video using the high frame rate video at 240 frames per second. Frame rate is an indicator of the video's quality captured by a camera. The high frame rate incurs smoother-looking transitions from one frame to the next, ensuring a higher level of details in the amount of captured motion, which includes tiny movements like breathing movements. In the second step, we select the region of 50 x 50 pixels around the abdomen or the shoulder and use the Gaussian filter to reduce the noise. We have considered the ROI in different sizes as 50x50, 100x100, and 150x150 in the empirical experiment and found that the 50x50 gives the best result. Then we continue to find the object of interest again in subsequent video frames. Specifically, the Minimum Output Sum of Squared Error (MOSSE) motion tracking is used to track the selected region of interest. The last step is to calculate the average pixel intensity in the selected region of interest. Signal filtering is the primary key process to acuratetly estimating the respiratory rate and representing breathing patterns. Therefore, the Butterworth filter, Filtfilter, and Saviszky-Golay filter are considered for smoothing waveform before counting the peaks. Moreover, the Findpeaks function provides the peak location of the input data by searching for the maximum local value of the sequence.

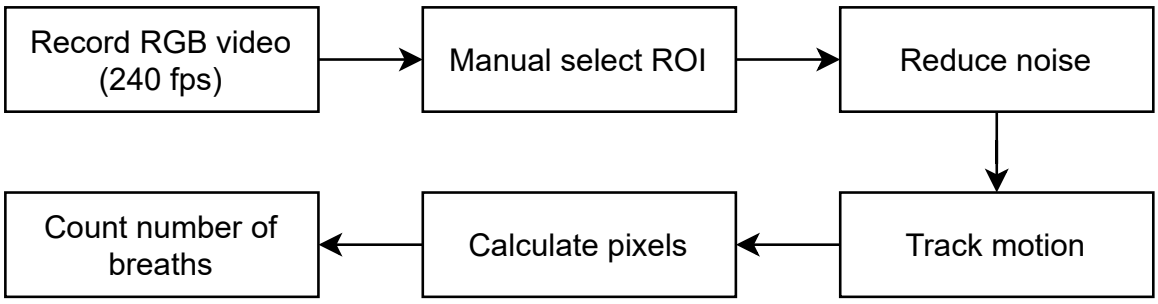

Figure 0-1:The proposed method (high frame rate video experiment).

ROI Selection

Like the related works described in Section 2.1, the respiratory rate can be counted by observing breathing movement. In this phase, the boundary of the subject's body laying down on the bed is focused on utilizing edge detection and thresholding technique to locate the area related to breathing movements. We manually test to select the region of interest on the subject's boundaries, as depicted in Figure 2.2, which shows the possible selected rectangles used to detect the breathing movement. The size of each ROI was set as 50 x 50 pixels and placed on the upper body. The characteristic of the selected area contains a part of the body and background. We calculate the accuracy of each ROI from P1- P11 to find the body area associated with breathing movement. For example, the clear points related to breathing movements that we can see with the naked eye are P5, P6, and P8, placed around the waist area. The selected region of interest and the accuracy of each ROI are shown in Figure 2.3. Breathing movements can be detectable in the raw signal of some waveforms as shown in Figure 2.4 (P5, P6, P9, P10).

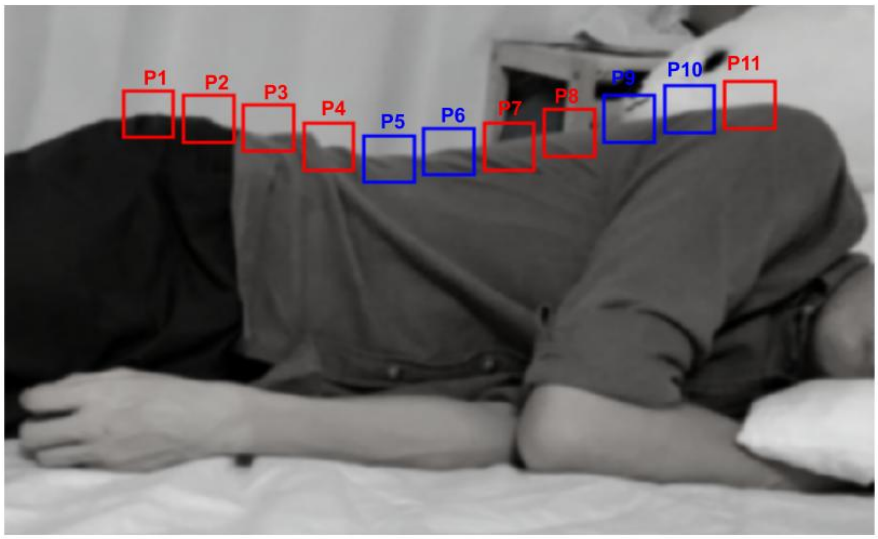

Figure 0-2: Manual ROI selection on the body edge.

The accuracy formula provides accuracy as a difference in error rate from 100% (2.1). The error rate is the percentage of the difference between observed and actual values divided by the actual value (2.2). The observed value is the number of breaths from the experiments, and the actual value is the number of breathings from ground truth data.

$$Accuracty = 100\% - Error\ Rate \quad (0.1)$$

$$Error\ Rate = \frac{|Observed\ Value - Actual\ Value|}{Actual\ Value} \times 100 \qquad (0.2)$$

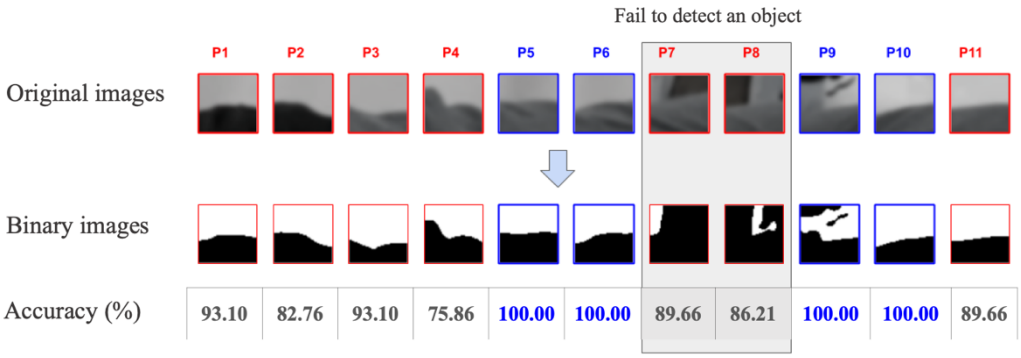

Figure 0-3: The depict of each ROI and its accuracy.

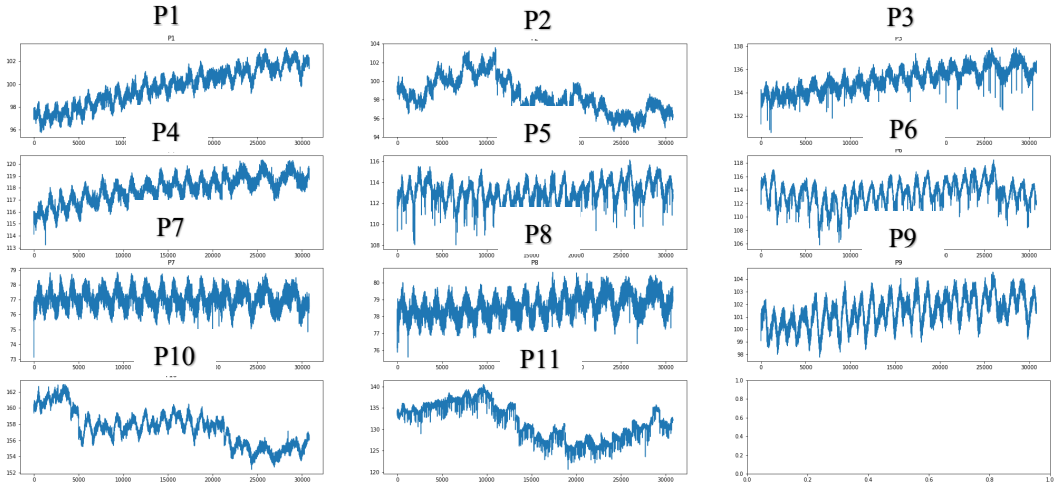

Figure 0-4: Plot of respiratory signal of each ROI.

As the above observation, we found that the ROI should be placed on the upper body's boundary and should contain the haft of background. Then we try to apply edge detection to locate the body boundary more precisely, as explained in Figure 2.5. Firstly, the Gaussian filter is used for smoothing the image. Second, the edge function has been performed. The detected edge is smoothed and is dilated with kernel 25 and iteration 2. Finally, we find the contour and draw a bounding box around the contour. There are multiple bounding boxes that are not related to the breathing movement. Figure 2.6 depicts all boundary boxes placed on the body edges using edge detection. The size of each box depends on the detected edges. Then, we calculate all candidate ROIs and manually select the best result, which gives the highest accuracy for each subject.

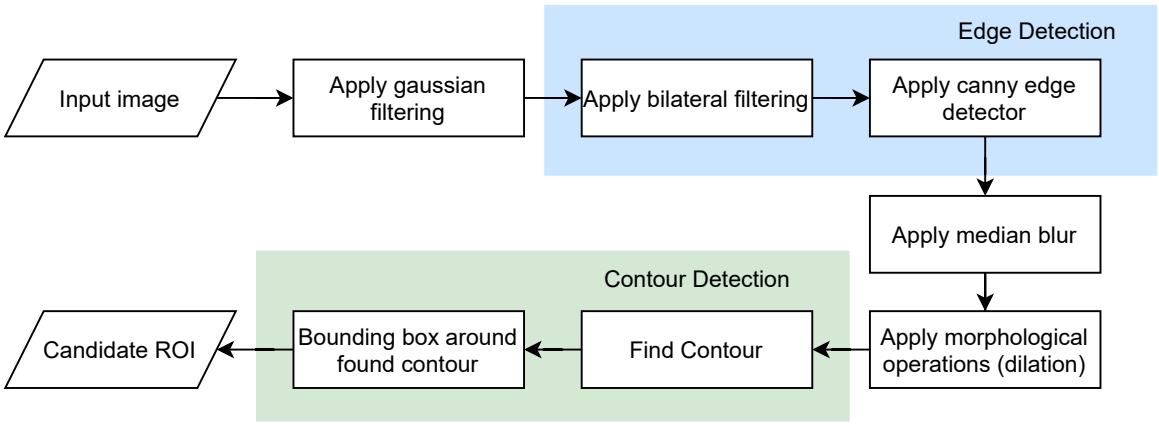

Figure 0-5: The ROI selection method.

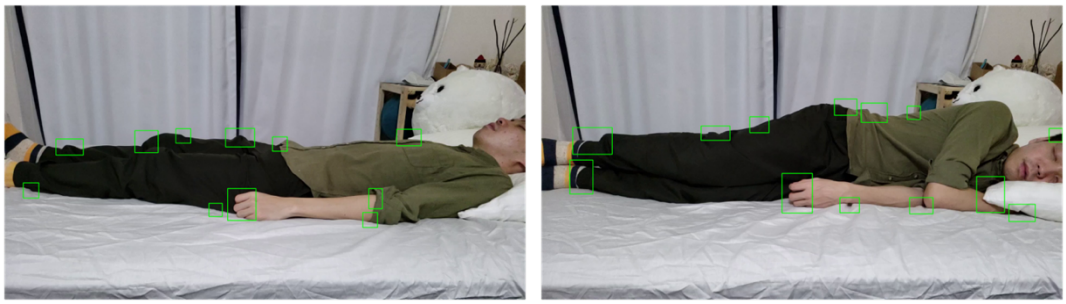

Figure 0-6: The sample output of candidate ROI selection based on edge detection.

Noise Reduction

After manual ROI selection, we applied the Gaussian filter to blur the image and remove noise in that ROI again. The Gaussian filter can remove noises in images due to light conditions. Then the signal is calculated as the average pixel intensity of the region of interest for each frame.

Motion Tracking

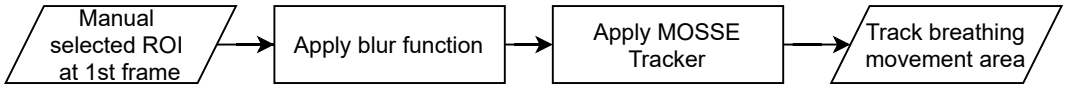

Figure 0-7: Breaths movement tracking process.

Motion tracking is the process of tracking the movement of an object within a region of interest area. The purpose of this process is to precisely locate a moving object in the video. The MOSSE motion tracking was compared as the empirical experiment with another object

tracking algorithm using the OpenCV library. The result shows that the MOSSE motion tracking is more suitable for our experiment. We take the initial set of object detection (breaths movement area) as an input set of bounding box coordinates. The MOSSE tracker uses an adaptive correlation filter to track the object [77]. The correlation is performed in the Fourier domain to make the computations faster. It is indeed robust and efficient computation with speed reaching several hundred frames per second. After the ROI is selected at the first frame, the ROI is cropped and the filter is initialized with the ROI set in its center. Then the filter is correlated with a tracking window in the video to find the new location of the object. Figure 2.7 shows the process of breath motion tracking.

Respiratory Extraction

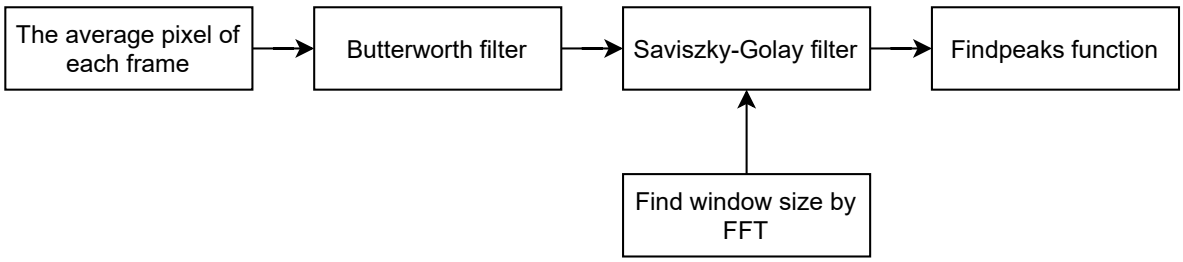

Figure 0-8: Respiratory estimation workflow.

The respiratory extraction workflow shows in Figure 2.8. Firstly, the ROI related to the breath's movement area was selected as a set of bounding box coordinates. We applied the blur function to reduce some noise and tracked that box. Next, at each frame f, the average intensity value is calculated for each ROI of each frame. Figure 2.9 exemplifies a gathered signal from the mean intensity of a selected ROI in a sequence of frames. Then the respiratory pattern is extracted using filtering operations. Thus, appropriate cut-off frequencies and bandwidth need to be defined. It is crucial to accurately design the filter parameters to obtain the proper performance of the measuring system. A 7^{th} order Butterworth low pass filter with a cut-off frequency in 1.5 Hertz, corresponding to 90 breaths per minute, was chosen to eliminate unreasonable frequencies unrelated to respiratory movements. Even after applying a low pass filter, the signal still has multi-peaks in one cycle, requiring smoothing signals. A Savitzky- Golay (SG) filter is a low pass filter that can be applied to a set of digital data for smoothing the data and increasing the data's precision without distorting the signal tendency [78]. The SG filter has two design parameters, i.e. the window length and the filter order. The optimal window length depends on the noise power, the number of samples, signal waveform, and filter order [79]. Figure 2.10 shows the smoothing results for a breathing pattern (red dash-dot line) in case of

using a third-order polynomial fit with 825 window length. The empirical experiment is executed to select the proper window length that provides higher accuracy for all subjects. Finally, we apply the Findpeaks function to obtain the input data's peak location by searching for the maximum local value of the sequence.

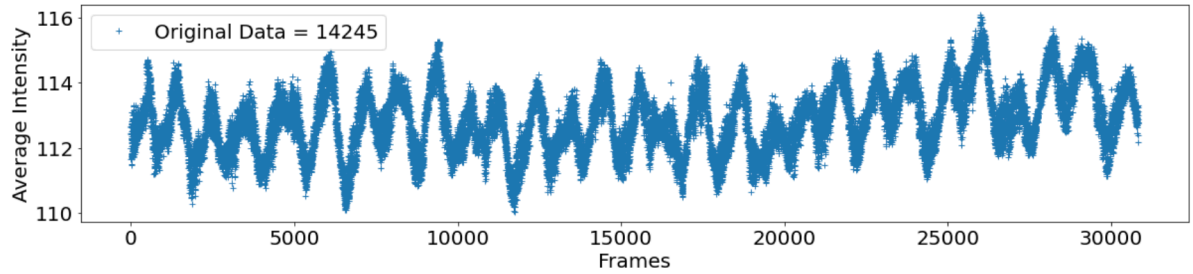

Figure 0-9: The sample of original breathing waveform.

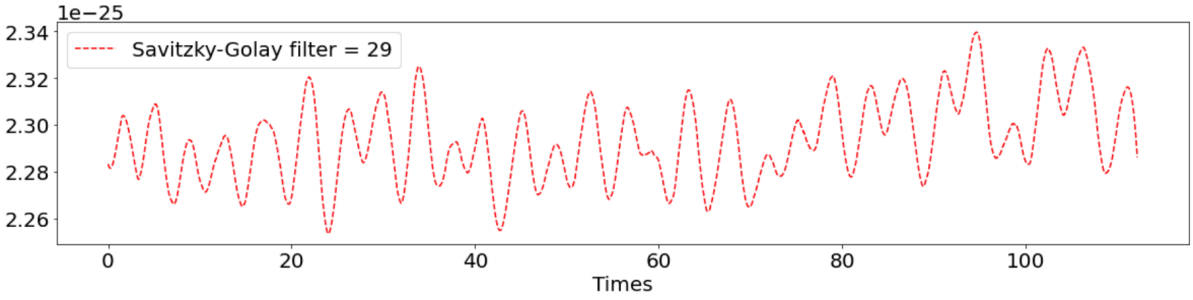

Figure 0-10: The sample of filtered breathing waveform.

2.2.2 Data Acquisition

Data were collected while volunteers were lying down on a bed in front of the smartphone camera (Galaxy S9+) at a distance of 0.6 meters. The smartphone is stabilized on the table by using the tripod to ensure that the camera was not affected by movement during the experiment. The experiments were carried out indoors and with a stable amount of light.

Data were collected from 9 volunteers (four females and five males) between 25 and 32 years old, each dressed in slim fit and dark clothes. The background view and bedcovers are white color. Although this is an unusual sleeping environment, we set this situation for the test with people who want to nap in the daytime and use their smartphones to monitor themselves. The volunteers are invited to lie down on the side of the bed and regularly breathing. The video was recorded with a built-in slow-motion mode for approximately 120-160 seconds. The resolution

is set at 1920 x 1080 pixels and saved in MP4 format. Table 2.1 shows the environmental setup details displayed in Figure 2.11.

The reference breaths are observed from the vertical rise and fall of the volunteer's waist or shoulder, and the number of torso rises is counted. One respiration consists of one complete vertical rise and fall of the torso or the inhalation cycle and exhalation of air. Breathing patterns obtained from the video signal show the shape of uphill and downhill graphs representing inhalation and exhalation clarity.

Table 0.1 Environmental Setup and Details.

Items	Description
Camera	Smartphone (Galaxy S9+)
Resolution	1920 x 1080
Frame Rate	240 fps
Distance	0.6 m
Number of Subjects	9
Color Depth	8-bit
Image Format	MP4
Low light Compensation	Disable
Ground-Truth	Observed

Figure 0-11: Environment setup of sleeping position.

2.2.3 Result of High Frame Rate Video Experiment

We use the Google Colab to implement the proposed method on image and signal processing. Figures 2.12-2.20 illustrate waveforms of the respiratory signal extracted from the recorded image of subjects in sleeping situations. Time durations in trials are between 134 seconds on average. The number of breaths refers to the number of peaks, corresponding to the number of breathing, is counted by the Findpeaks function.

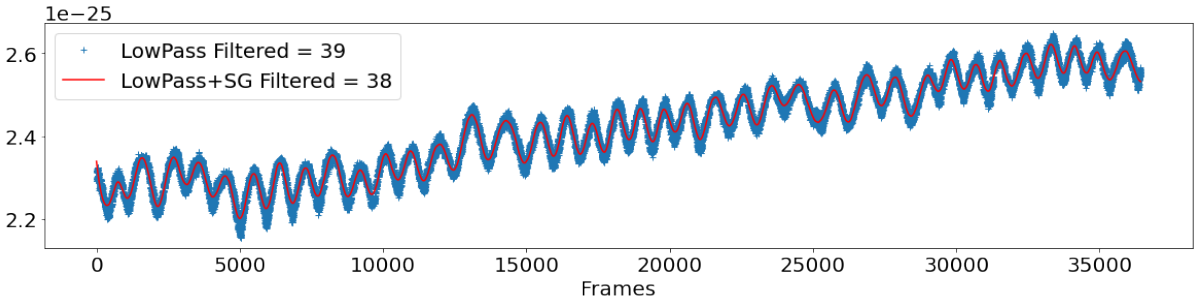

Figure 0-12: The breathing pattern of subject No.001.

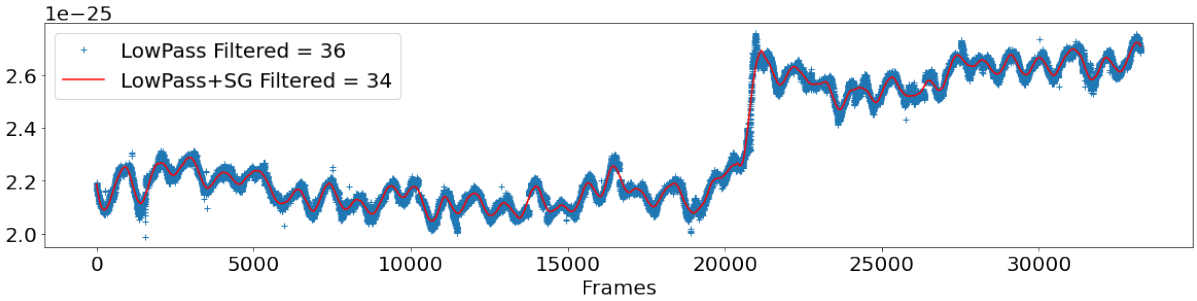

Figure 0-13: The breathing pattern of subject No.002.

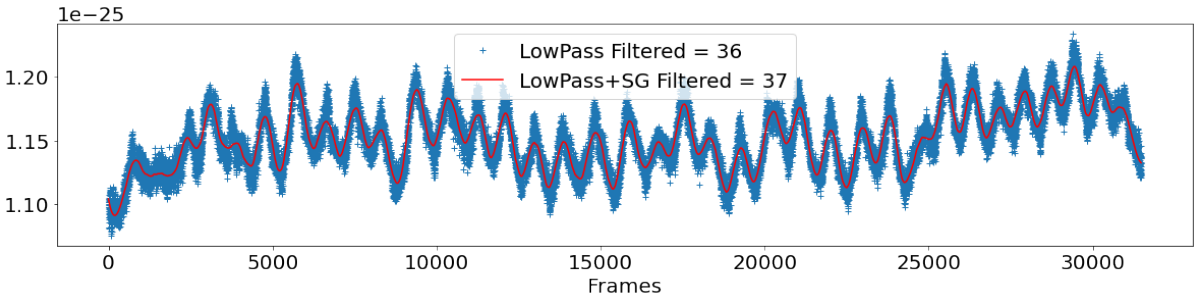

Figure 0-14: The breathing pattern of subject No.003.

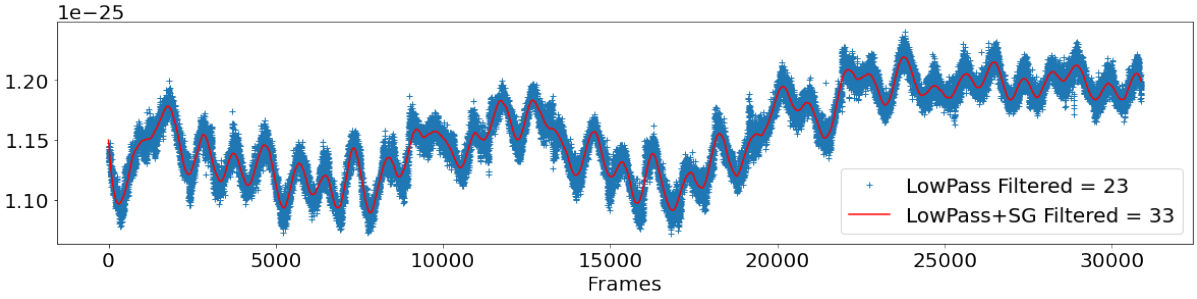

Figure 0-15: The breathing pattern of subject No.004.

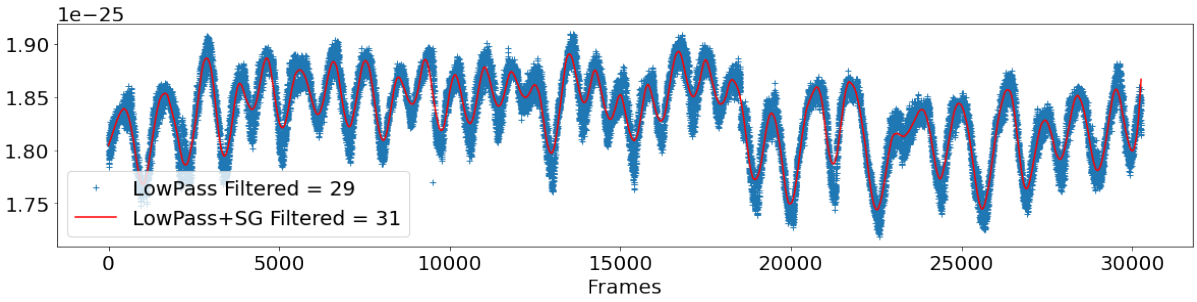

Figure 0-16: The breathing pattern of subject No.005.

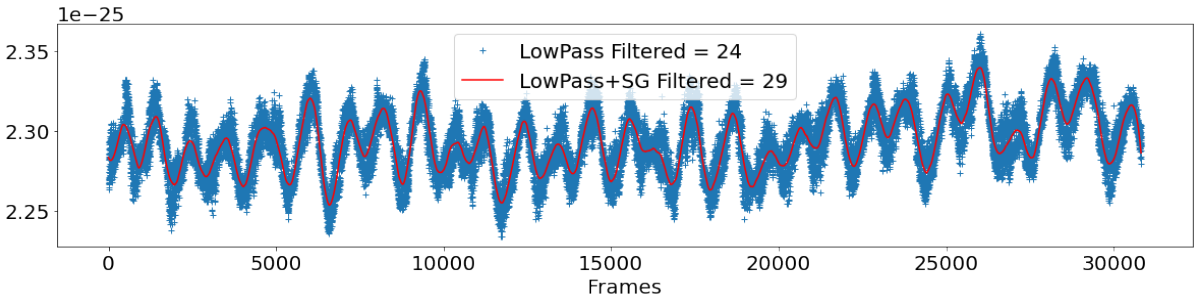

Figure 0-17: The breathing pattern of subject No.006.

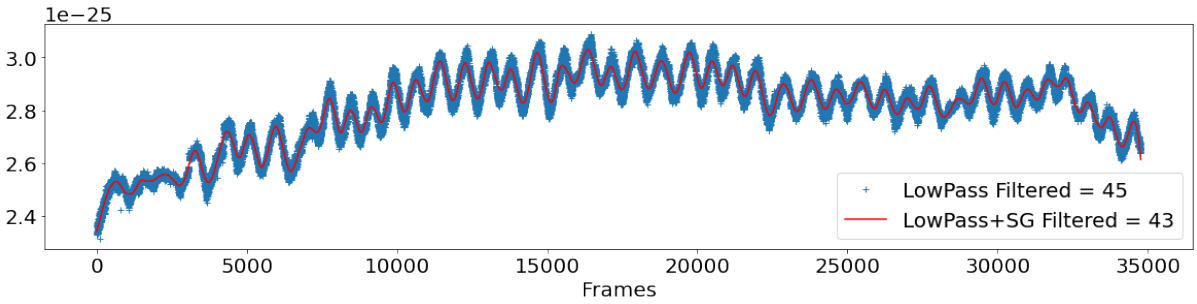

Figure 0-18: The breathing pattern of subject No.007.

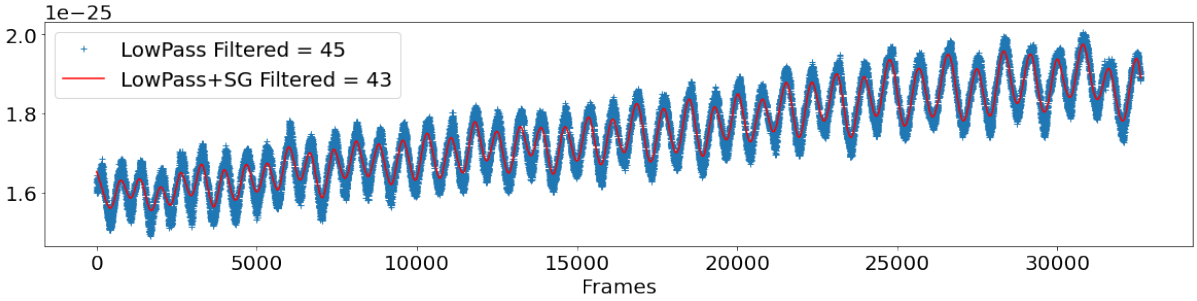

Figure 0-19: The breathing pattern of subject No.008.

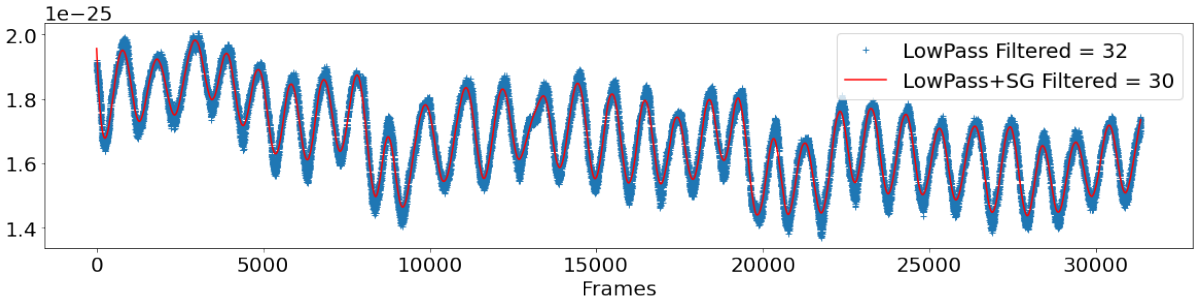

Figure 0-20: The breathing pattern of subject No.009.

Table 0.2 The result of the reference number of breaths comparing the experiment.

Subject No.	Duration (secs)	FPS	Reference Breaths (times)	Number of peaks		Accuracy (%)	
				LowPass	LowPass+SG	LowPass	LowPass+SG
001	151.63	240.27	39	39	38	100.00	97.44
002	138.37	240.23	35	36	34	97.14	97.14
003	130.99	240.27	36	36	37	100.00	97.22
004	128.55	240.18	33	23	33	69.70	100.00
005	125.98	240.23	31	29	31	93.55	100.00
006	128.27	240.27	29	24	29	82.76	100.00
007	144.72	240.24	43	45	43	95.35	100.00
008	135.68	240.27	43	45	43	95.35	100.00
009	130.47	240.24	30	32	30	93.33	100.00
Average	**134.962**	**240.24**				**91.91**	**99.09**

The high frame rate experiment results are summarized in Table 2.2, compared with the reference breaths. Subject 06 has reference breaths 29 times, and when applied only LowPass filtered, breaths are counted as 24 times because some peaks are not prominent or have a small width. The LowPass filter followed by the SG filter is applied, giving more apparent prominence with a smoother waveform. The result gives 29 peaks are counted, although the waveform is not stationary. As for the result of all subjects, when applied only to the lowpass filter, the average accuracy is 91.91 percent. Besides, the average accuracy after the applied proposed approach is 99.09 percent, where 100% accuracy is obtained for six of nine subjects. This result confirms that the SG filter for smoothing signals provides high accuracy.

2.3 Ordinary Video Experiment

As we discussed in Sect. 2.2, the smartphone camera is a simple device that is used daily. However, the slow-motion video required a high computation for processing. Therefore, this section uses a regular smartphone camera to record ordinary video at 30 fps in the bedroom, and the subjects are covered by a black blanket. Additionally, this section presents an automatic ROI selection for respiration estimation in sleeping positions, which utilizes a human detection method to remove unrelated breathing movement signals to improve respiratory estimation accuracy. This experiment aims at individual continuous monitoring at home to screen the cessation of breathing while sleeping.

2.3.1 Proposed Method

This experiment investigates the automatic selection of the relevant area to extract respiratory signals from RGB video. Operations with automatic ROI selection are described in Figure 2.21.

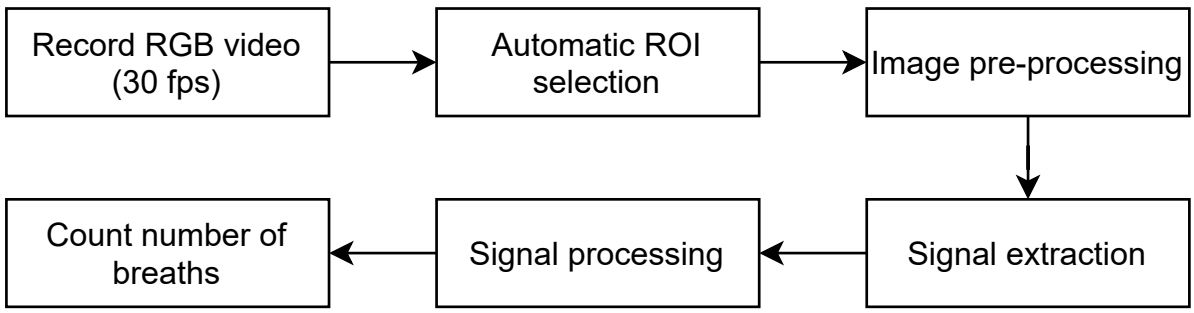

Figure 0-21: The proposed method (ordinary video experiment).

RGB Video

The RGB video input is converted to grayscale pixels by calculating the weighted sum of the corresponding red, green, and blue pixels as (2.3).

$$Y = 0.2125\ R + 0.7154\ G + 0.0721\ B \qquad (0.3)$$

Gaussian blur [76] is used to remove the noise from the frames in order to avoid interference with the experimental results. Then, our ROI selection method utilizes a motion detection method to locate the movement area that relates to the breathing movement in the video. The breathing movement is generally very tiny and cannot be seen with the naked eye. In video image processing, the motion would be detected by examining the difference in pixel values between consecutive frames. The breathing movement area is located in the first ten seconds (300 frames) of the video to ensure at least one breath cycle is included.

ROI Selection

In this experiment, we compare the different ROI sizes, including whole frame, human detection, and ROI selection. First, the Mask R-CNN [76] was applied to locate the human in sleep position. This step features a cropping method to limit the observation area by removing the unwanted areas at the beginning frame. Then, the image from the video capture is imported into the Mask R-CNN model built on ResNet101 to locate the person area. Finally, pre-trained models based on the COCO dataset are used to detect a person. As a result, the Mask R-CNN detects a human in a sleeping position, lying on the back and lying on the side, as shown in Figure 2.22. The sleeping person in an image and the bounded box around them are detected. Boxes, masks, class scores, and labels are drawn in the left figure. There are three objects detected in this figure with their scores of the human body (0.768), bed (0.943), and human head (0.896).

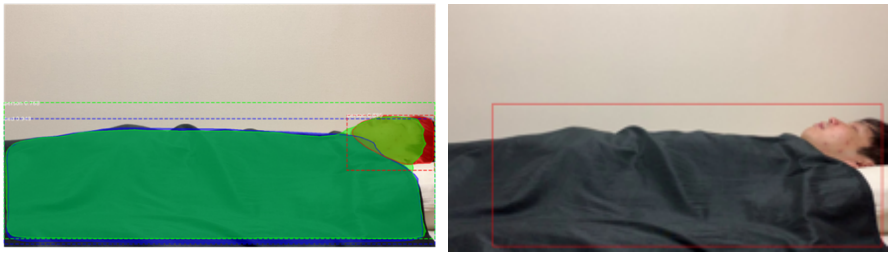

Figure 0-22: The human detection through Mask-R-CNN (left), The ROI of human detection (right).

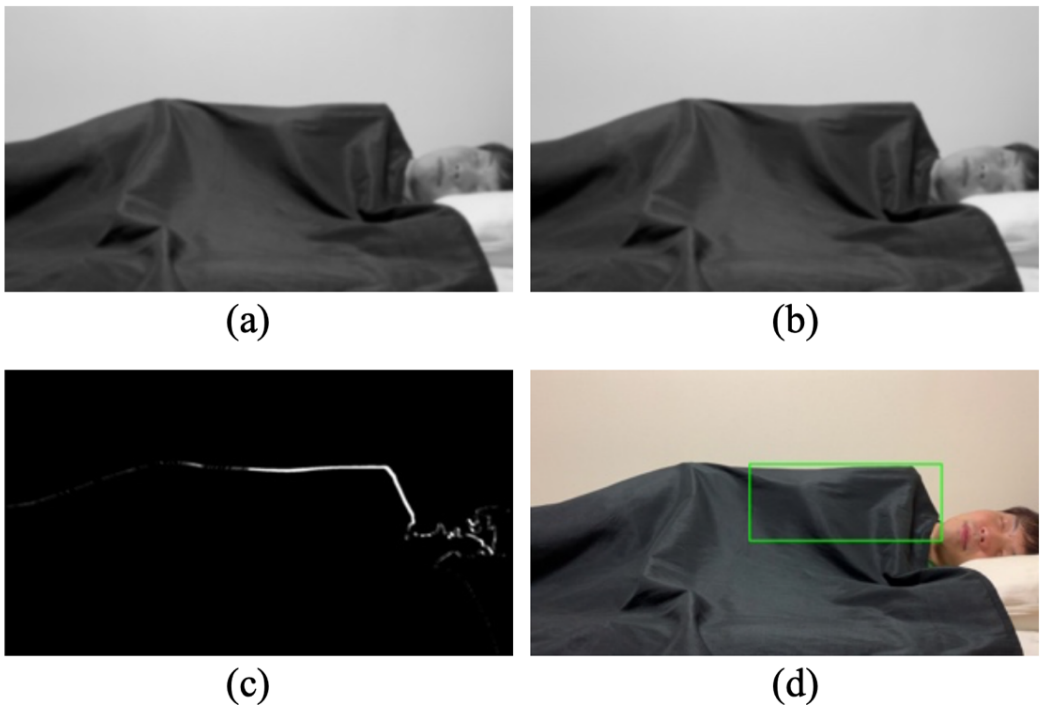

Figure 0-23: Frame x (a) and frame y (b) both after noise removal are used to compare the difference between frames. (c) is a binary image of different images (a) and (b). (d) shows the located breathing motion area.

The comparison of selected areas is executed based on the Structural SIMilarity (SSIM) index, that is a method for measuring the similarity between two images [80]. SSIM measures the perceptual difference between two similar images to determine the (x,y) coordinate difference. First, we calculate the SSIM by using (2.4) between frames and then select two frames, i.e. SSIMmax and SSIMmin, representing the maximum and the minimum values of SSIM. Next, these two frames (Figure 2.23 (a) and Figure 2.23(b)) are used to calculate the difference between two similar images by using the SSIM method again. This is because the largest value between those two frames may indicate the breathing movement. Next, the threshold method is applied to create the binary image in which a white pixel indicates the difference, as shown in Figure 2.23 (c). Finally, the white pixel area is set to ROI by the bounding box using the contour function (see Figure 2.23 (d)). Obtained three different ROI sizes are depicted in Figure 2.24, where blue represents the whole frame, red is the human detection result, and green is used for ROI.

$$SSIM(x,y) = \frac{(2\mu_x\mu_y + C_1)(2\sigma_{xy}+C_2)}{(\mu_x^2+\mu_y^2+C_1)(\sigma_x^2+\sigma_y^2+C_2)} \quad (0.4)$$

The SSIM measure between two windows x and y of common size $(N \times N)$ with μ_x is the average of x, μ_y is the average of y, σ_x^2 is the variance of x, σ_y^2 is the variance of y, σ_{xy} is the covariance of x and y.

Figure 0-24: Display the subjects with a region of the whole frame (blue), human detection (red), and the ROI selection (green).

Image Pre-processing

After the bounding box of ROI is set, the next step is signal extraction by converting RGB images to grayscale pixels to calculate the weighted sum of the corresponding red, green, and blue pixels (2.3). Then uses the Gaussian blur filter to remove noise in the ROI area.

Respiratory Signal Extraction

We compare three signal generation methods among varoius signal extraction methods as the difference between frames, the average pixel values, and the white pixel count for each frame. In addition, the ROI selection (proposed method), human detection, and the whole frame are compared. Equation (2.5) is the function from the scikit-image used to compute the score and difference between two grayscale images. The score represents the structural similarity index between the two input images. The difference image contains the actual image differences between the two input images that we wish to visualize.

$$score, difference = compare\_ssim(Frame_n, frame_{n+1}) \quad (0.5)$$

Let P be a set of pixels in a frame, the average pixel values are calculated by (2.6), and the white pixel is counted by (2.7) where white pixel value (x) is 255.

$$Average\ of\ pixels = \frac{\sum_{x \in P} x}{|P|} \quad (0.6)$$

$$Count\ white\ pixel = \sum_{x \in P | x=255} 1 \quad (0.7)$$

Respiratory Signal Processing

The obtained respiratory signals retrieved above are smoothed before applying signal processing based on the scipy.signal.findpeaks package. Then we count the number of peaks corresponding to the number of breaths. A 6th-order bandpass Butterworth filter [81] with a lower cutoff frequency of 0.05 Hz and a higher cutoff frequency of 1.5 Hz, which are equivalent to 3-90 breaths per minute, is used. Next, we use the SG filter [82] to smooth the respiratory signals by applying a 3rd order polynomial and a window length of 71, which is decided based on preliminary experiment research. Formula (2.8) calculates the percentage error to measure the error between the ground truth value and the measured value. The number of peaks refers to the measured value, and the ground truth value is the number of breaths counted manually from the video by the three persons.

$$Percentage\ Error = \frac{|Measured - Groundtruth|}{Groundtruth} \times 100 \quad (0.8)$$

2.3.2 Data Acquisition

Our experiment uses a smartphone camera (iPhone XS) to record video sequences at the frame rate of 30 fps and an image resolution of 1920 × 1080 pixels. The video was recorded for approximately 80 seconds and saved in RGB, MOV raw format. Volunteers were invited to lie down on a bed in front of the camera. The distance between the camera and the volunteers was approximately 0.60 meters. The smartphone was stabilized using a tripod to ensure the camera was not affected by any movement during the experiment. The experiments were performed indoors and with a stable amount of light. Data were collected from nine volunteers (five females and four males) between 25 and 32 years old whose BMIs ranged from 18.36 to 25.73 kg/m^2. They were covered with a thin black blanket, and the temperature of the room was kept

at 27–29°C. The background view was a light-colored wall. The ground truth breathing signal was obtained from a thermal camera (Seek Thermal CompactPRO) with a 320 × 240 thermal sensor to monitor the subjects' noses.

Table 0.3 Environment setup and details.

Items	Description
Camera	iPhone XS
Resolution	1920 x 1080
Frame Rate	30 fps
Distance	0.6 m
Number of Subjects	9
Color Depth	8-bit
Image Format	MP4
Low light Compensation	Disable
Ground-Truth	Observed

Table 0.4 Subjects detail.

Subjects	Weight (kg)	Height (cm)	Gender	BMI
01	59.00	168	M	20.90
02	47.00	160	F	18.36
03	60.00	169	M	21.01
04	52.70	167	F	18.90
05	55.00	160	F	21.48
06	47.50	157	F	19.27
07	57.50	168	M	20.37
08	77.00	173	F	25.73
09	75.00	180	M	23.15

2.3.3 Result of Ordinary Video Experiment

Table 2.5 shows the accuracy of the respiratory rate obtained by three signal extraction methods; the difference of frame, average pixels, and count number of white pixels. Each method was tested in two sleeping postures and three region sizes, including whole frame, human area detection, and ROI detection. The results show that the accuracy of the average pixels method is the highest at 98.80% (lying on the back) and 93.21% (lying on the side). The proposed method also had the highest accuracy in both sleeping positions when estimated by the average of pixels.

Table 0.5 The accuracy of respiratory rate extracted from different method.

Signal Extraction Methods	**Accuracy (%)**					
	Lying on the Back Posture			**Lying on Side Posture**		
	Whole Frame	**Human Detected**	**Proposed Method**	**Whole Frame**	**Human Detected**	**Proposed Method**
Difference of frame	90.78%	90.19%	88.24%	88.68%	90.61%	92.82%
Average pixels	89.28%	95.41%	98.80%	87.46%	92.56%	93.21%
Count white pixel	86.42%	87.78%	87.29%	89.00%	91.75%	88.70%

Then we explain the result of each subject with the average pixels method in Table 2.6 in which the ground truth value is obtained by manual counting of the breathing. From this table, it is clearly seen that the performance of the proposed method is better than that of the whole frame and human detection for all sleeping positions. An ROI can be detected more precisely for the lying on the back position than the side position. With the lying on the side position, an ROI around the arm area caused more errors than that around the chest area (i.e., subject005, subject006, and subject009).

Table 0.6 The result of average pixels method of each subjects.

Video	Ground truth (#breath)	Measured value (#breath)			Accuracy (%)		
		Whole Frame	Human Detection	ROI selection	Whole Frame	Human Detection	ROI selection
001-back	27	24	27	27	88.89	100.00	100.00
002-back	15	19	18	14	73.33	80.00	93.33
003-back	16	16	16	16	100.00	100.00	100.00
004-back	19	17	18	19	89.47	94.74	100.00
005-back	21	19	21	21	90.48	100.00	100.00
006-back	14	12	13	14	85.71	92.86	100.00
007-back	14	13	14	15	92.86	100.00	92.86
008-back	21	20	20	21	95.24	95.24	100.00
009-back	24	21	23	23	87.50	95.83	95.83
001-left	26	24	26	26	92.31	100.00	100.00
002-left	19	20	20	20	94.74	94.74	94.74
003-left	16	15	15	15	93.75	93.75	93.75
004-left	19	18	18	18	94.74	94.74	94.74
005-left	17	22	20	15	70.59	82.35	88.24
006-left	21	19	20	20	90.48	95.24	95.24
007-left	18	25	23	21	61.11	72.22	83.33
008-left	17	17	17	17	100.00	100.00	100.00
009-left	19	21	19	18	89.47	100.00	94.74
		Average of lying on back side position			**89.28**	**95.41**	**98.00**
		Average of lying on left side position			**87.46**	**92.56**	**93.86**
		Average all position			**88.37**	**93.98**	**95.93**

The results of ROI selection and breathing waveform of each subject are shown below. The sample ROI of each subject shown in the photo is in a fixed position for all frames that we located from the breathing motion area. Besides, the waveform is depicted by calculating the average pixel within each frame's ROI.

Table 0.7 The result of selected ROI and breathing pattern for each subject.

Subjects	Lying on the side	Lying on the back
001	 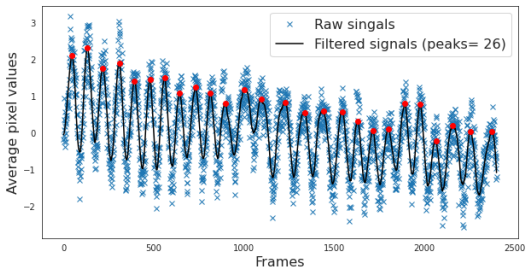	 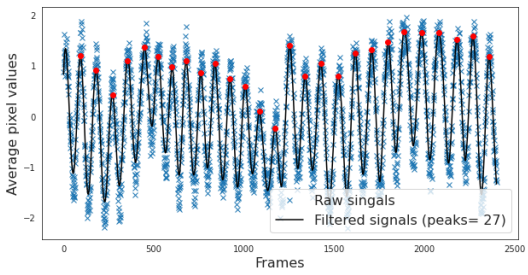
002	 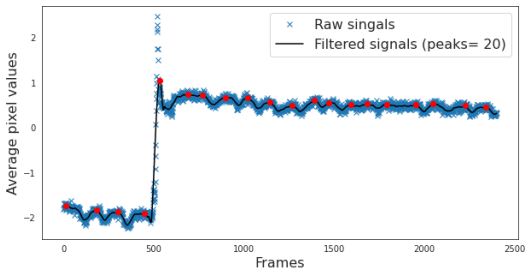	 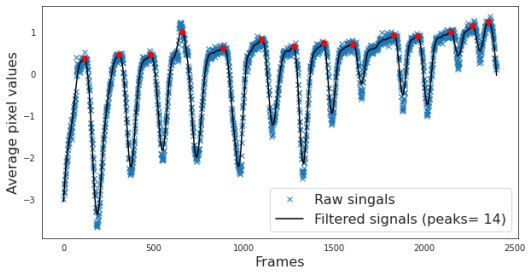

Subjects	Lying on the side	Lying on the back
003	 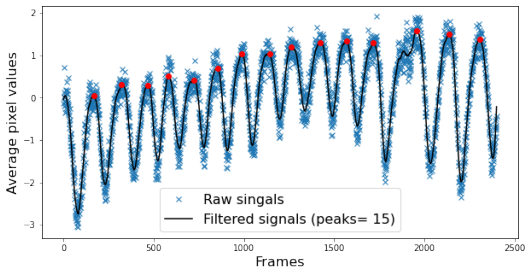	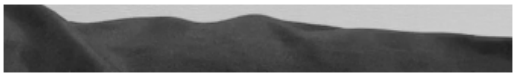 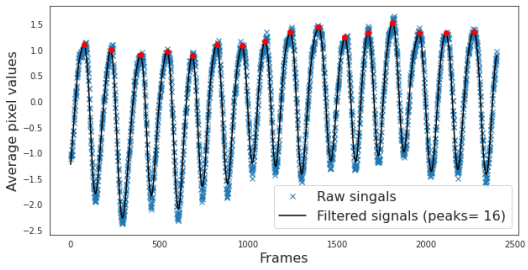
004	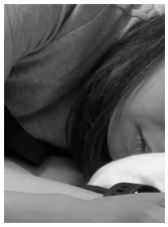 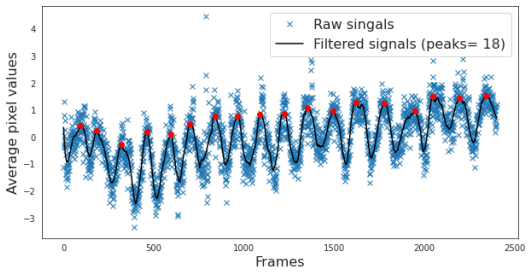	 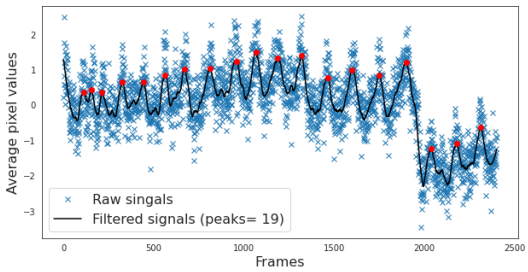
005	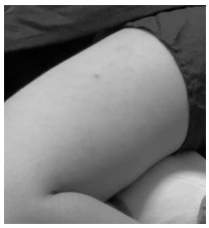 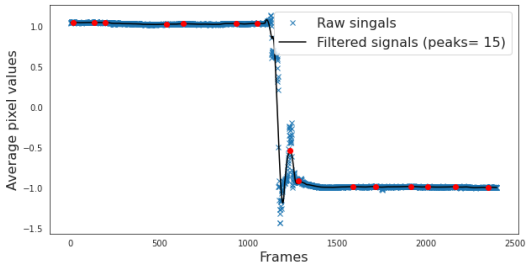	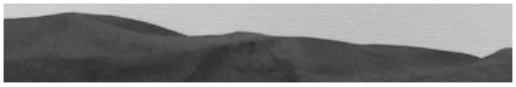 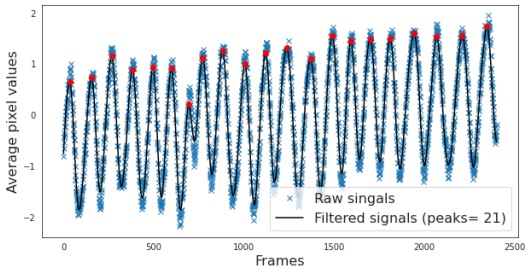

Subjects	Lying on the side	Lying on the back
006		
	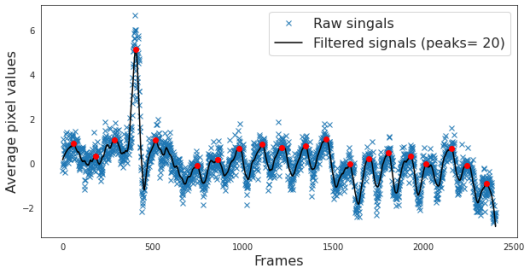	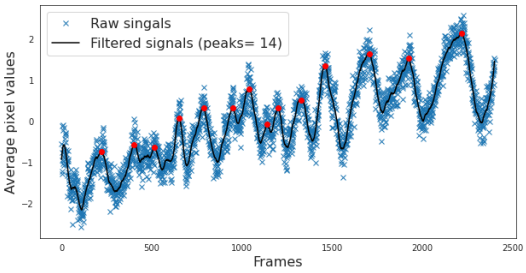
007		
	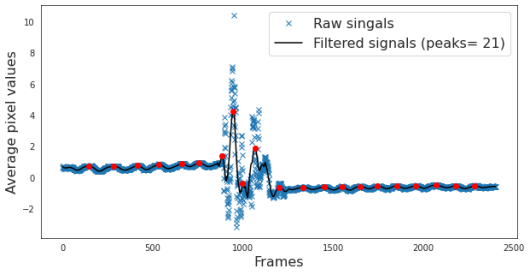	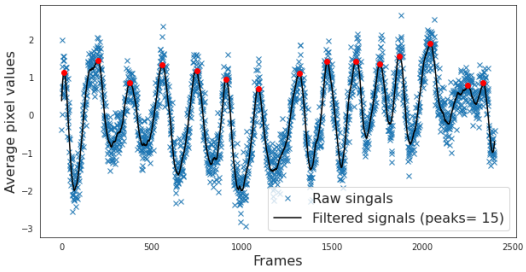
008		
	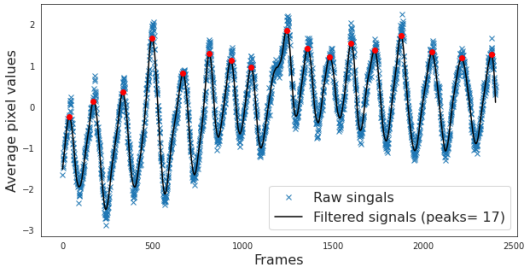	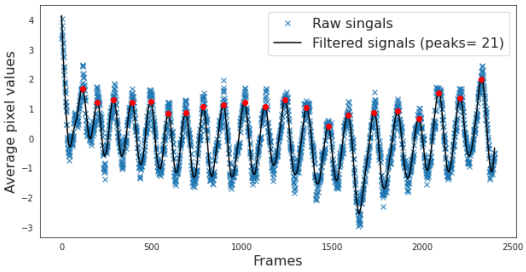

Subjects	Lying on the side	Lying on the back
009	 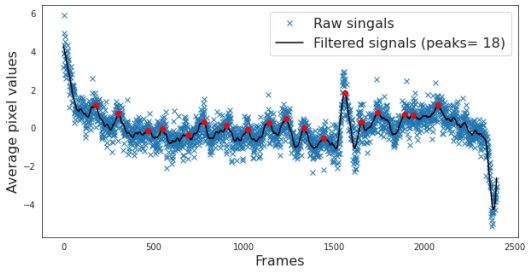	 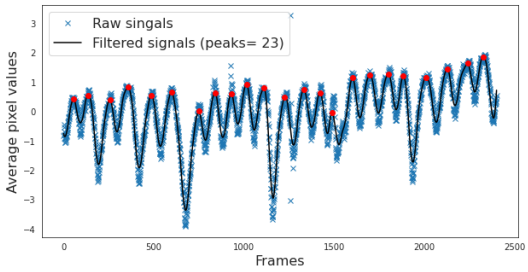

The scatter plot and linear regression results of the reference and measured respiration rates are presented in Figure 2.25. A strong correlation was found in the proposed method ($R^2 = 0.914$), as the data points (green line). The human detection technique showed a positive relationship ($R^2 = 0.807$). The whole frame technique had a low relationship ($R^2 = 0.500$). These results demonstrate that the proposed method is effective for respiratory measurement.

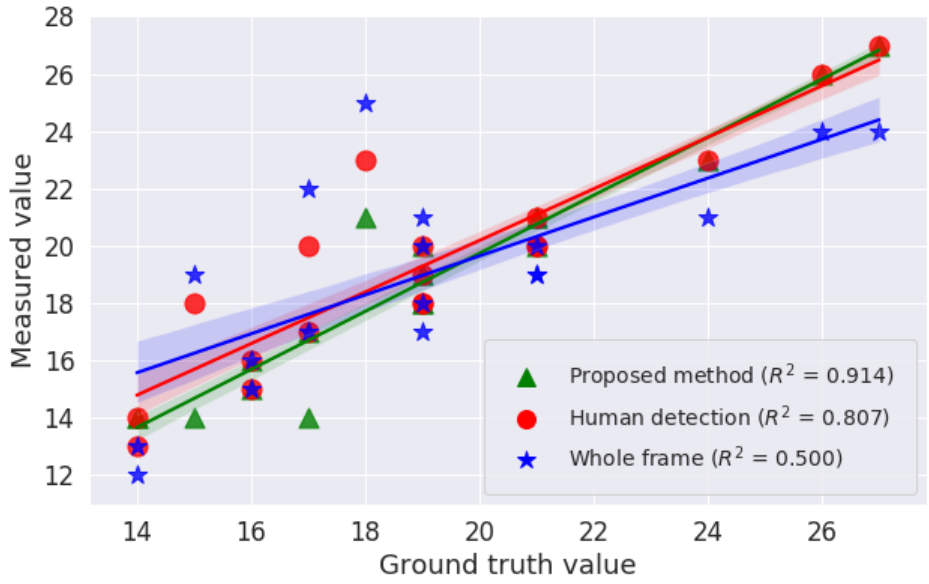

Figure 0-25: Scatter plot of the ground truth value and measured value.

2.4 Discussion

In order to investigate the performance of high frame rate video and ordinary video experiments, we have shown the ROI selection methods to estimate the respiratory in a sleeping position. In the experiments, the respiratory signal is collected in two different conditions; i.e. the subjects covered with a blanket and without a blanket. In the high frame rate video experiment, the proposed method focused on the boundary between the body and the background, which may depend on the postures or clothing patterns of the subjects. Assuming that the spatial features are correctly selected, this method is simple and effective. Although it is not the ideal sleeping environment, this study confirms that ROI is essential in acquiring respiratory information from images. Then, we consider changing the experiment environment by covering the subject with the black blanket in the ordinary video experiment. Besides, we applied the Mark R-CNN to detect the human body in sleeping postures, comparing it with the ROI selection method based on motion.

The limitations of this study include the video recording of the breathing while the volunteers were lying down and instructed not to move, as found in other non-contact optical approaches [30]. Additionally, in this study, we evaluated the performances of the proposed system only in the quiet breathing range and in a limited population. We also found the many factors that affect the breathing estimation based on the non-contact optical approach described below.

Varying Motion Patterns

There are various kinds of motions of a subject, such as a limb movement, jaw and face movement, head/neck or trunk movement, rotation, translation, and body shaking. In the experiment, we found a motion of the background seriously affects the performance. The non-respiratory motions should be recognized and to be removed when estimating the respiratory signal. Abnormal movements are also associated with wakefulness or sleep.

Varying Clothing and Blanket Pattern

The clothing and blanket pattern may directly affect respiratory ROI detection. The slim-fit and loose-fit clothes influence the data quality and validity of the video-based methods. The clothing and blanket pattern degrades the edge detection performance, which creates the wrong position not related to breathing motion. In the first experiment, the background view and cloth pattern are detected by using the edge method which some areas are not related to the body and breath movements. Then, we used a dark, non-patterned blanket covering the subject to reduce

the edges that were not involved in breathing in the second experiment. Besides, we select ROI by motion detection technique to estimate the more accurate respiratory.

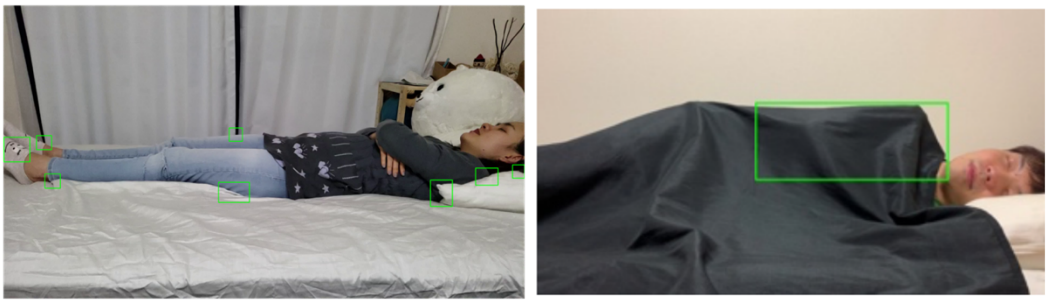

Figure 0-26: Example of candidate bounding boxes.

Varying Sleeping Positions

The sleeping position is uncontrollable in the natural sleep environment. In experiments, the volunteer was asked to lie down on the bed with no movement. In the first experiment, we manually selected the ROI, and in the second experiment, we applied the image processing algorithm to select the ROI. However, it still has a limitation when the volunteer moves or changes their posture. Therefore, the ROI cannot be set in the first frame but must be automatically located and usually updated when the subjects change their posture. The uncontrolled sleeping posture challenge is the accurate locating of the related breathing area in the sleeping position.

Varying Frame Rate Video

The frame rate is thus the number of frames displayed per unit of time, and it is measured in frames per second that consists of a sequence of photos displayed at a specific rate to show motion. High frame rates are good for slow-motion video because we capture the image with more stills, whereas a high frame rate requires ample storage. High frame rate video also takes longer than ordinary video to process images due to many frames. However, the results have similar accuracy.

2.5 Summary

This chapter discussed respiration monitoring based on smartphone cameras to obtain the subjects' video when lying on the bed. The first experiment lies in the high frame rate video at 240 fps, and the second experiment uses an ordinary video at 30 fps. Both experiments show

that the accuracy was similar, but the high frame rate video takes a long time to process due to numerous images. The main factor affecting the number of peaks on the waveform depends on the breath's movement area. It is more challenging when the subjects are in a sleeping position. The solution is limiting the observed area was also presented by using ROI selection. We present a manual ROI selection for a high frame rate video to prove the highest related area and the condition that affects accuracy. Experimental results showed that the subject body's boundaries as the shoulder, chest, and abdominal are mainly related to the breathing movement area. The background and cloth patterns also affect the performance of image processing when locating the subject body's boundaries. In the ordinary video experiment, we controlled the background view and covered the subject with a black blanket to solve the problem. The automatic ROI selection and ROI size have been discussed in this study.

Chapter 3
Non-Contact Respiration Monitoring based on Thermal Camera

To possibly apply the vision-based non-contact respiration monitoring in the real sleeping environment with a dim light and uncontrolled sleeping position, a thermal camera may detect respiration in this environment, where each subject lies on a bed naturally in a home. This chapter aims to integrate the analysis of respiration and body movements. Since respiratory signals and that of body movement are related to common sleep disorders, such an approach can provide comprehensive information that aids diagnosis.

3.1 Introduction

The breathing patterns during sleeping are utilized to identify the sleep disorder as sleep apnea, including obstructive sleep apnea (OSA), central sleep apnea, and complex sleep apnea syndrome. Sleep apnea is a cessation of the airflow that occurs when breathing repeatedly stops and starts during sleep, resulting in decreased oxygen flow to the brain and the rest of the body. Sleep apnea is generally characterized by the cessation of breath for at least 10 seconds during sleep [83]. The well-known index used to indicate the severity of sleep apnea is the Apnea-Hypopnoea Index (AHI), which counts the number of apnea events per hour. Besides, sleep monitoring can detect periodic limb movement disorder (PLMD), which is repetitive cramping or jerking of the legs during sleep. Patients with PLMD may suffer from daytime sleepiness, daytime fatigue, trouble falling asleep at night, and difficulty staying asleep throughout the night [84]. Usually, patients with PLMD are unaware of their leg movements unless their bed

partner tells them. It is also reported that movements are repetitive and rhythmic and occur every 20-40 seconds [85].

Thermal imaging is a rapidly evolving technology that is now turning up in hospitals, airports, and even homes. Respiratory can be monitored through thermal imaging [86]–[99]. Thermal imaging cameras rely on microelectromechanical sensors to produce an image from heat; the human body stands out from the surrounding field because it gives off more heat. The thermal image-based method has an advantage under varying illumination conditions and can reduce privacy issues. Previously, several approaches have been proposed to monitor respiration with a thermal camera by detecting the temperature change around the nostrils [37], [89], [91], [93]–[96], [99] or the airflow [90], [97], [98] in seated positions. They set the nose or the mouth as the region of interest (ROI) that can be defined manually or automatically by using anatomical features integrated with tracking algorithms [37], [93]–[96]. These approaches are performed by simulated breathing scenarios that the researcher designed, i.e., regular breathing, fast breathing, and hold breathing [93], [94], [96], [99]–[101]. The excellent result showed when they took the experiments in a controlled room in terms of temperature, humidity, and lighting. However, nose detection during sleep is still unsuccessful at all monitoring times.

In the sleeping position, the thermal-based method is an effective technique to measure the nasal airflow patterns [51] and has been utilized to detect sleep apnea [52], [102], analyze sleep activity [103], to classify body posture [104] during sleep for assisting the diagnosis of sleep disorders or evaluation of the quality of sleep. The studies using thermal imaging to monitor respiration in sleeping positions are reviewed in Table 3.1. Usman et al. [52] adopted thermal imaging to detect sleep apnea and study various breathing patterns. They used the Kanade–Lucas–Tomasi tracking algorithm to track a manually selected nose region. The result showed that 16% of a subject's head position did not allow correct identification of the region of interest at the nostrils. Therefore, this method was only possible with minor head movement without changing position. The automatic ROI selection was used to locate the nostrils, the tip of the nose, and the mouth area [15], [105], [106]. That ROI requires a tracking algorithm and works well without large head movement under a controlled environment. Abbas et al. [51] developed respiration monitoring for neonatal intensive care units by manually selecting the ROI around the nostrils of an infant.

Table 0.1 A research review of the thermal imaging-based method for respiration monitoring of sleeping position.

Authors	Subjects	Exp Duration	Controlled Env	Simulated Breathing	Selection /Detection	ROI localization	
						Area	Tracking
Usman et al.	Adult	5 min	Yes	Yes	M	Nostrils	Yes
Fei el al.	Adult	60 min	Yes	No	A-S	Nostrils	Yes
Al-Khalidi ei al.	Children	2 min	Yes	No	A-S	Tip of the nose	Yes
Hu et al.	Adult	10 min	Yes	Yes	A-S	Nose, mouth	Yes
Abbas et al.	Infant	2 min	Yes	No	M	Nostrils	No
Pereira et al.	Infant	5 min	No	No	A-D	N/A	No
Lorato et al.	Adult	2 min	Yes	Yes	A-D	N/A	No

M: Manually, A-S: Automatically Selection, A-D: Automatically Detection.

Most techniques work well when the nose is clearly visible in the image. On the other hand, the measurement was not feasible when the nose is outside the camera's field of view, a blanket blocks the nose, or the subject has large head movements. Recent works from Pereira et al. and Lorato et al. [107], [108] detected the respiration signal without the use of anatomical features. They selected the ROI containing the respiration information by using the Signal Quality Index. However, they did an experiment in a controlled environment in a short period that was not a real environment. Moreover, the motion artifacts are still a significant drawback of this algorithm. It was suitable for monitoring infants in neonatal care who did not have large movements.

This section aims to develop a measuring system capable of non-contact monitoring of respiration and body movements in natural sleep environment using a thermal camera. The natural sleep environment implies uncontrolled sleep posture, darkness, and covered subjects with a blanket. The proposed method for respiration monitoring and body movements detection is described. An overview of the proposed method is depicted in Figure 3.1. The input of the proposed method is the thermal video obtained under dark light. The Gaussian filter is applied to the input images as the pre-processing so as to remove noises from the input. The main part of the proposed method is composed of respiration monitoring and body movements detection,

each of which utilizes image processing and signal processing techniques in order. Details of these processes will be written below.

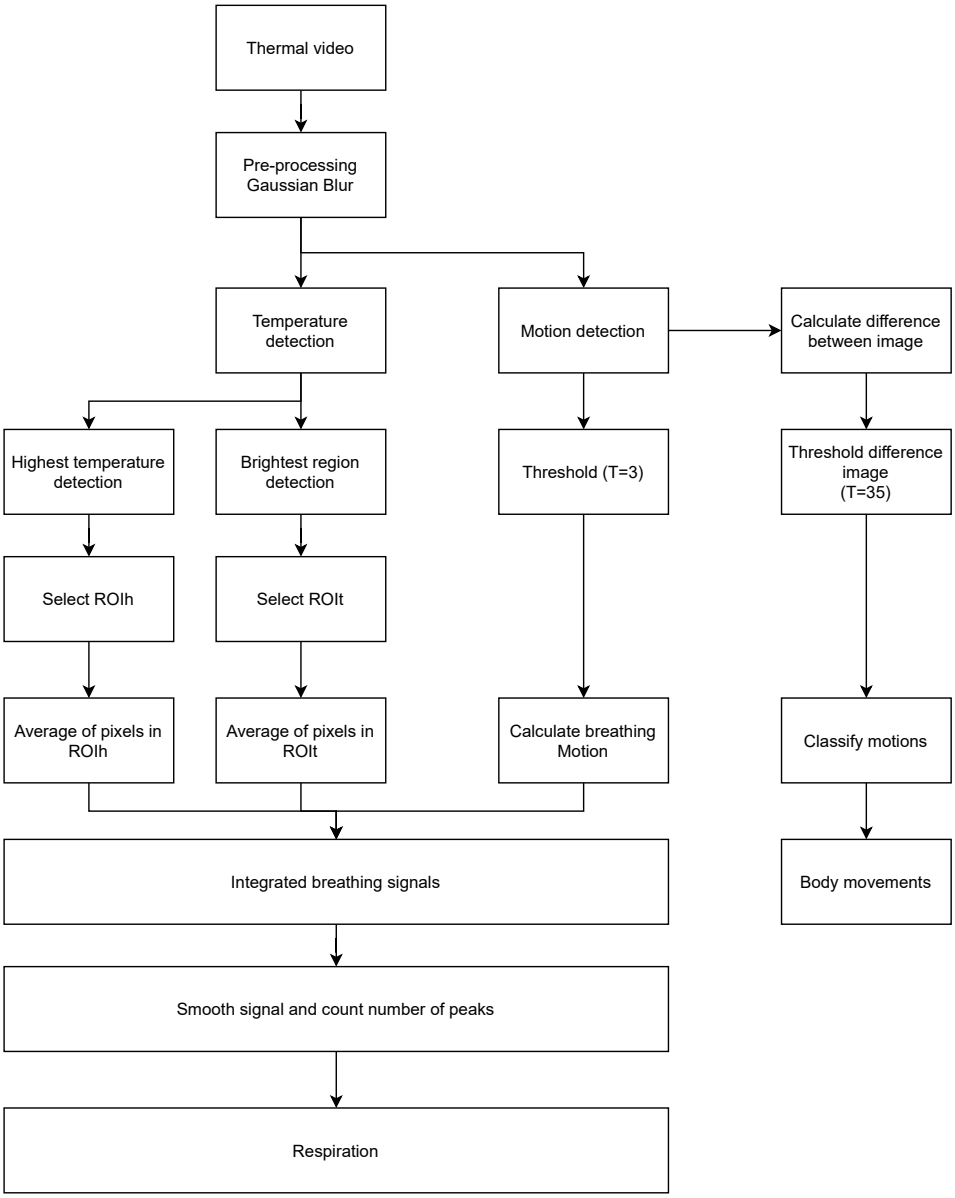

Figure 0-1: Proposed method.

3.2 Respiration Monitoring

The proposed respiration monitoring method contains an automatic detection of ROI by finding the highest temperature point and the largest portion of the high-temperature area and a

breathing motion detection. The temperature information is used to find the area of the breath while the breathing motion corresponds to the airflow and body movements presented by breathing. The respiration signals are extracted by integrated automatic ROI detection and breathing motion detection. Then the signal processing is applied to calculate the respiratory rate.

3.2.1 Automatic ROI Selection

We employ an ROI detection to limit the observation area, extracting important information to raise the accuracy of the respiratory estimation. Determining a suitable ROI position with proper size is also important. In a real sleep monitoring environment, it is not easy to detect a face or nostrils as an ROI because of the uncontrolled sleep posture, and the fixed camera position may make a face that does not appear in the camera view on some occasions. Besides, when the subject changes the sleep posture, ROI should be updated to the new location for which some research applied a tracking algorithm. The tracking algorithm works well with an apparent object but sometimes fails to track the nose or mouth in a sleeping posture. We propose an ROI detection on the thermal image in a sleeping position that does not require a tracking algorithm. Two different ROI detections are considered in this section, 1) the highest temperature point detection and 2) the largest portion of high-temperature area detection.

The highest temperature point detection

The highest temperature point is detected by using minMaxLoc, a function of the OpenCV [109] libraries that return the minimum and maximum intensities found in an image with their (x, y) coordinates. It is assumed that the maximum pixel intensities of the thermal image refer to a human's heat signature that is not covered by a blanket. The maximum pixel intensities found in the image correspond to the highest temperature of the body. We set the pixel to the center of the observation area. Then we draw a rectangle around the pixel, with the size of the square $N \times N$ pixels depending on the original frame resolution. In [14], the authors compared the ROI size of 10×10, 25×25, 50×50, 100×100, and 150×150 pixels. They found that the size of the ROIs for respiratory rate estimation is usually smaller than that for heart rate estimation. Therefore, in this study, we consider the three different ROIh sizes as 10×10, 25×25, and 50×50, as shown in Figure 3.2. The result of empirical research has shown that the 50×50 pixels provided the highest accuracy in accordance with the original frame resolution of 640×480.

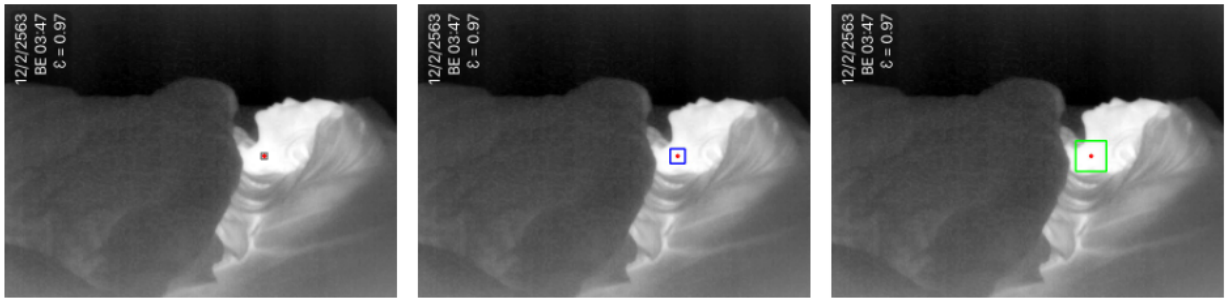

Figure 0-2: The sample of three different ROIh sizes as 10× 10, 25×25, and 50×50 (red point indicates the highest temperature point).

The largest portion of high-temperature area detection

Assuming that the human skin area indicates high temperature than other parts, the largest portion of the high-temperature area is detected by using the thresholding method. Thresholding is the method of segmenting the object from the background, finding the thresholds to segment the image into regions. This method is based on a threshold value to turn a grayscale image into a binary image. The suitable threshold value needs to be determined, and then the image can be segmented by comparing the pixel properties with these thresholds value. If the image intensity $I(x, y)$ is less than the threshold value, the image pixel is replaced by a black or white pixel if the image intensity is greater than the threshold value.

The threshold image $g(x, y)$ can be defined as (3.1) [110]:

$$g(x,y) = \begin{cases} 1 \ \ if \ I(x,y) \geq \ T_R \\ 0 \ \ if \ I(x,y) < \ T_R \end{cases} \qquad (0.1)$$

To determine the threshold value T_R, we coordinated empirical research with varying values among 128, 144, 160, 176, 192, 208, and 224. It was confirmed that the T_R value 176 is the one that yielded the best results in all the performed tests.

Figure 3.3 (a) shows the segmentation of the input image with the thresholding method. Then, we used the findContours function of the OpenCV library to find the location of white regions that return the outlines corresponding to each of the white blobs on the binary image. The bounding box is drawn around those contours (see Figure 3.3 (b). Finally, we find the most prominent contour and bounding box around that contour, as shown in Figure 3.3 (c). In this study, we selected the biggest box as ROIt.

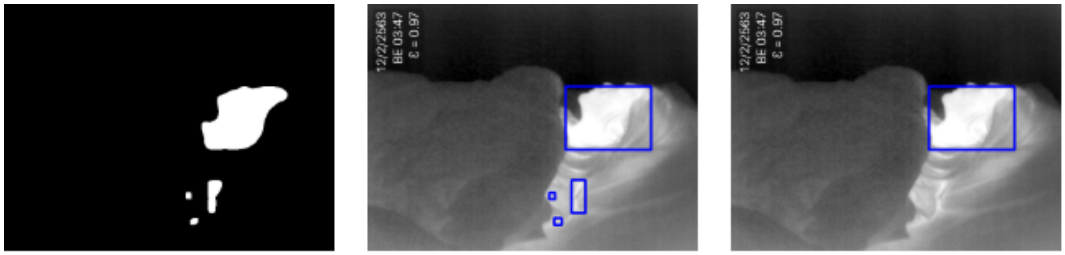

(a) (b) (c)

Figure 0-3: (a) All contours, (b) bounding rectangles around all contours, and (c) bounding rectangle around the most prominent contour.

Then ROIh and ROIt are cropped to extract signals $\overline{s}_h(f)$ and $\overline{s}_t(f)$ by computing the average of pixel values (3.2) within each ROI of each frame, where $S(x, y, f)$ is the pixel value of the thermal image at pixel (x, y) in the video frame f , N_* is the vector of pixel coordinates in ROIh or ROIt, and n_* is its number.

$$\overline{s}_*(f) = \frac{1}{n_*}\sum_{x,y\in N_*} S(x, y, f) \quad (0.2)$$

3.2.2 Breathing Motion Detection

Breathing motion detection applies a subtraction method for detecting the motion by calculating the difference between two frames. Specifically, the absolute difference for all pixels between the current frame $I(x, y, f)$ and the frame one second before $I(x, y, f - s)$ is calculated (3.3):

$$B(x, y, f) = |I(x, y, f) - I(x, y, f - s)|, \quad (0.3)$$

where s is the frame rate.

Then, we extract portions of the moved area by using thresholding, erosion, and dilation operations. Parameters used in these operations are 5 for thresholding pixel value difference and 5×5 kernel for opening (i.e., erosion and dilation). Next, bounding boxes are determined by finding contours by filtering out small movements as noise. Finally, the number of bounding boxes is counted as the metric of breathing motion (BM), as shown in Figure 3.4.

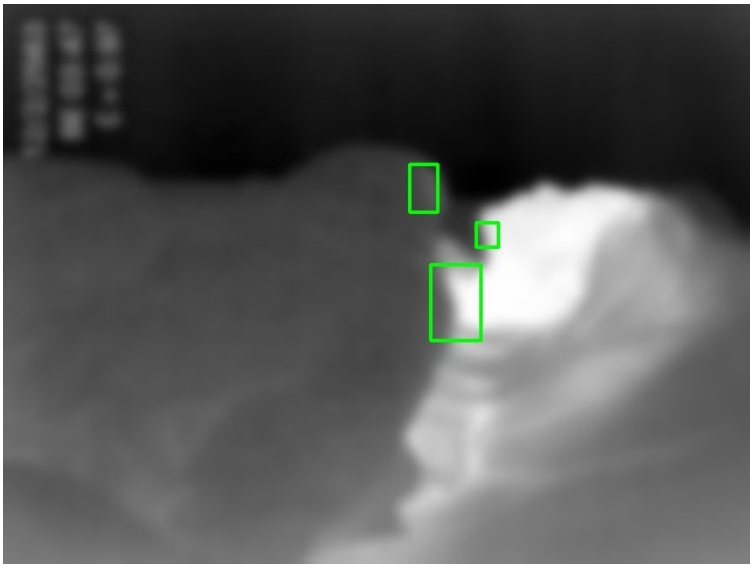

Figure 0-4 The bounding boxes around the breathing motion.

3.2.3 Respiration Signal Analysis

There are three respiration signals extracted by using ROIs based on temperature detection and breathing motion detection. Steps to estimate the respiration signals are described as follows. The respiration signals can be extracted by detecting the chest movements, breathing airflow, and the temperature change around the nostrils. However, a specific method does not always detect the above phenomena in sleep monitoring due to the fixed camera position. An independent subject posture may make the region out from the camera view. In such a case, an alternative method for respiration detection is required. We assume that respiration can be detected by mixing the temperature change of ROIs and breathing motion. Therefore, we combine three signals by employing the root mean square (RMS) to calculate the average of the respiration signals as (3.4).

$$Respiration\ signals = \sqrt{ROIt^2 + ROIh^2 + BM^2} \quad (0.4)$$

The 3rd order Butterworth bandpass filter [111] with a lower cutoff frequency of 0.05 Hz and a higher cutoff frequency of 1.5 Hz was applied to the respiratory signals. The frequency bound is equivalent to 3-90 bpm, based on the typical RR for an adult person (12-20 bpm) and monitoring the abnormal RR that is less than 12 bpm and higher than 20 bpm.

The SG filter is a least-square polynomial filter that reduces noises while retaining the shape and height of waveform peaks [112]. Here, the SG filter was used to smooth the signal after the bandpass filter. The SG filter's output increased the precision of the data without distorting the signal tendency. There are two parameters of the SG filter, including window length and

the filter order, which closely relate to the filter's performance. In this study, we tested the parameters and selected the optimal values to get the best-filtered signal, i.e., the window length of 51 and the polynomial order at 3rd were used. The result of the SG filter still includes small peaks, and thus a moving average is calculated to detect only the desired peaks and ignore small ones.

The fusion signal in Figure 3.5 (a) was smoothed by the SG filter and moving average calculation (see Figure 3.5 (b)), and then the number of peaks was counted. Figure 3.5 (c) depicts the peaks detection of the experiment signal, followed by the peak detection of the reference signal in Figure 3.5 (d), which are assumed to reflect the number of breaths. The findpeaks function is used with adjusting its width to 10 based on empirical research.

The number of peaks is calculated as breaths per minute (bpm) for each 60 seconds slice of input video (1020 samples at 17 fps) and was compared with the reference RR. For performance comparison, the accuracy of the RR estimation was tested using the RMSE defined as (3.5).

$$RMSE = \sqrt{\frac{1}{N}\sum_{i=1}^{N}\left(x_i^{exp} - x_i^{ref}\right)^2} \qquad (0.5)$$

where N is the total number of the slices, and x_i^{exp} and x_i^{ref} represent the experimented and reference RR values obtained for slice.

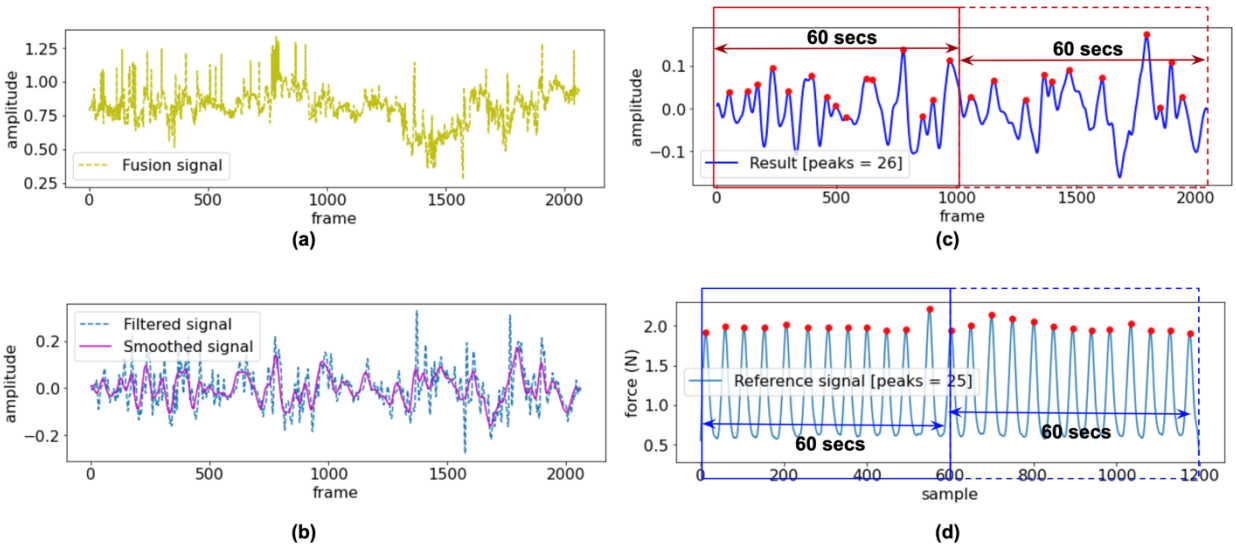

Figure 0-5: (a) Sample of fusion signal, (b) filtered and smoothed signals, (c) peak detection of experiment signal, and (d) peak detection of the reference signal.

3.3 Body Movement Detection

This process aims to determine more significant action than the respiration representing a big movement like limb movement, head movement, and full position change during sleep. First, an absolute difference image $B'(x, y, f)$ between adjust two thermal images $I(x, y, f)$ and $I(x, y, f-1)$ is obtained by $B'(x, y, f) = |I(x, y, f) - I(x, y, f-1)|$ Then, we binarize the difference image by thresholding method.

In the same manner as the breathing motion detection, we extract portions of the moved area by erosion and dilation operations. While using 35 for the thresholding value in order to detect large body movements, the same parameters are used for erosion and dilation. Then, we apply the findContour function to examine whether those are a portion of the moved area. If any contour is found, the body movement signal is set to 1. An example output of the body movement is shown in Figure 3.6.

Figure 0-6: Sample output of the body movements detection.

3.4 Experimental Results

This section analyzes the signal gathered in two experiments. Experiment (1) is the respiration monitoring, and experiment (2) is the body movements detection during sleep. The results were compared with the reference signals obtained by the Go Direct Respiration Belt.

We assessed the performance of our proposed non-contact monitoring of respiration and body movement detection under natural sleep environments. During the experiments, the thermal videos were captured using a portable thermal camera (Seek Thermal Compact PRO for

iPhone) attached to a smartphone and fixed on a tripod in front of a participant located at approximately 100 cm. The camera was set at the proper position so that the upper body of a participant was apparent in the camera's field of view. The Seek Thermal Compact PRO is a highly portable thermal imaging camera with a wide, 32-degree field of view. This thermal camera has a resolution of 640 x 480 pixels and detects infrared wavelengths in the spectral range of 7.5 to 14 Microns. The camera's emissivity was set to 0.97, as this is suitable for human skin temperature measurement. Besides, the videos were recorded at 17 frames per second (fps). The Go Direct Respiration Belt was used as a reference to collect human respiratory effort and respiratory rate from a force sensor and an adjustable nylon strap around the chest during respiration. The measuring parameters were set to 10 samples/s, and the duration was approximately 5,400 seconds. Figure 3.7 illustrates an environment setup.

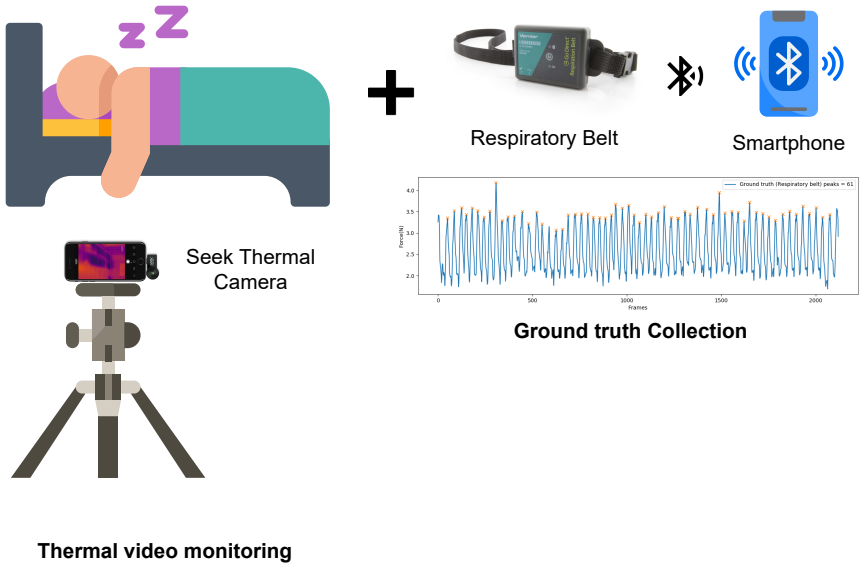

Figure 0-7: Environmental setup.

The data were collected on different days, from multiple camera positions with volunteers wearing different clothes. The experiments were conducted under real-life conditions, and volunteers were invited to record in their rooms while they were sleeping. They placed a respiratory belt around their ribs and mounted a thermal camera on a tripod by themselves before they went to bed. Sixteen healthy people with ages between 25 years old and 37 years old (29.88 $\pm$ 3.26 years old), ten females and six males, with heights between 151 cm and 180 cm (162.63 $\pm$ 7.37 cm), with weights between 47 kg and 78 kg (57.38 $\pm$ 9.28 kg), and body

mass index (BMI) between 18.65 kg/m^2 and 27.64 kg/m^2 (21.64 $\pm$ 2.98 kg/m^2) volunteered for this experiment.

Breathing Pattern Monitoring

The breathing pattern signal is obtained from ROIh, ROIt, and breathing motion. There are two ROIs shown in Figure 3.8 that were identified for every frame. The red rectangle is the bounding box around the highest temperature point; the blue rectangle is the significant portion of the high-temperature area. The ROIh locates on the subject's skin, preferably at the highest body temperature point, has a smaller size. The most oversized box is detected by the thresholding method as the ROIt. The size of detected ROIt is dependent on the contour area. Then ROIh and ROIt are cropped to extract the signal by computing the average pixel values within each ROI of each frame.

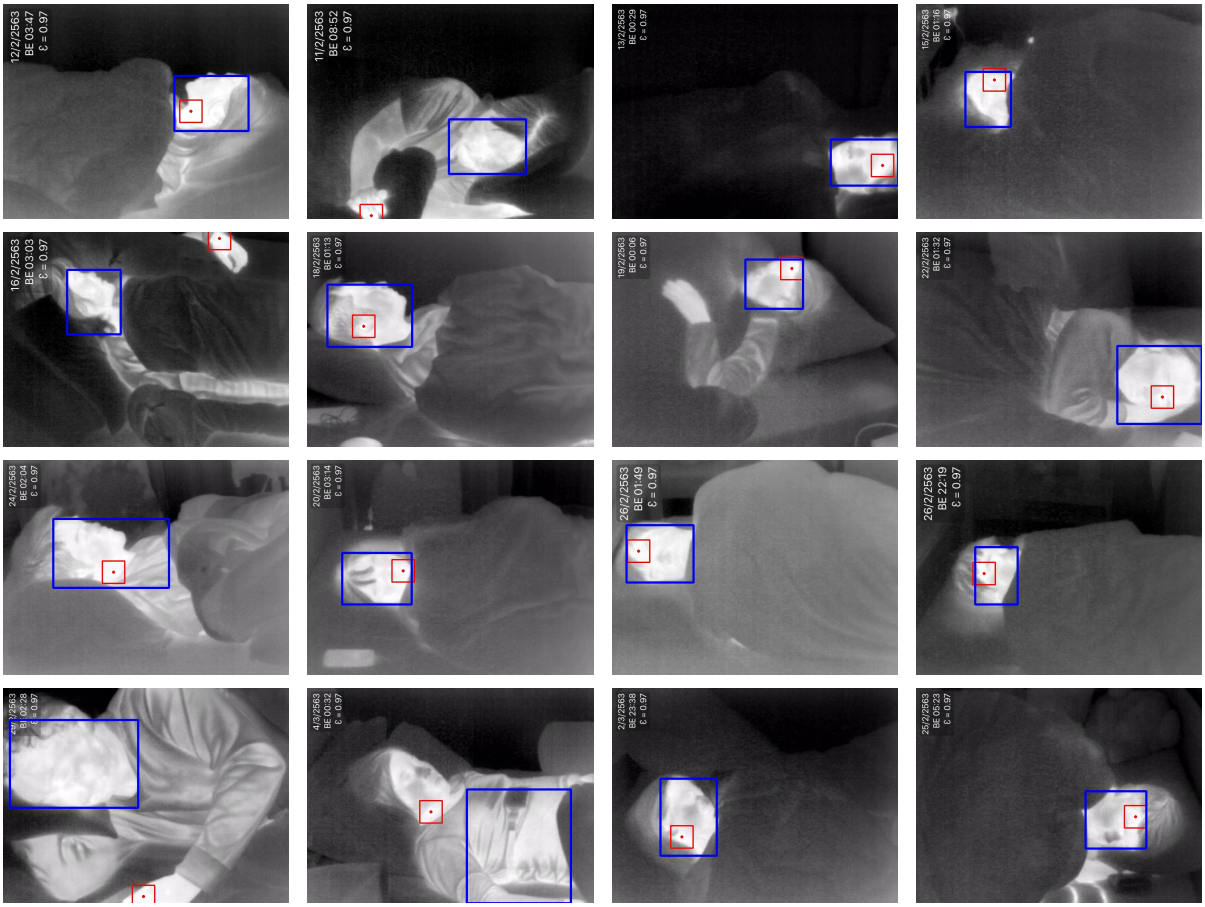

Figure 0-8 : The sample result of selected ROI.

Table 3.2 summarizes the results obtained for all subjects, including respiratory rate estimation and body movement detection. The respiratory rate estimated by our proposed method was

compared with the reference signal obtained by the respiratory belt. The RMSE was calculated by considering all the breaths in each signal collected during the experiment minute-by-minute. The average respiratory rate in the overall subjects is 14.78 ± 1.93 bpm in the reference signal and 14.47 ± 0.60 bpm with the proposed approach. The standard deviation of RMSE for the respiratory rate of all subjects is 0.75 bpm, and the average is 1.82 bpm. The small RMSE indicates that the proposed approach is robust for the subject's variation. As for body movement detection, we counted the number of movements, the number of frames including body movement, and the total duration of body movements.

Table 0.2 The result of respiratory rate estimation.

Subjects	**All duration(secs)**	**Respiratory rate (bpm)**			**Body movements**			
		Reference RR	**Experiment RR**	**RMSE**	**#Movements**	**#Frames**	**Duration (secs)**	**Degree**
S01	5371.05	12.71	14.05	1.56	14	269	15.69	1.12
S02	5397.94	13.69	14.22	1.11	15	199	11.65	0.78
S03	5379.37	16.75	14.78	2.20	7	63	3.69	0.53
S04	5192.31	12.23	13.37	2.00	35	642	37.86	1.08
S05	5212.78	17.62	14.39	3.32	9	200	11.72	1.30
S06	5200.51	16.45	14.48	2.23	9	214	12.53	1.39
S07	5332.39	14.38	14.36	1.47	16	218	12.80	0.80
S08	3495.39	14.65	14.29	1.18	15	749	43.48	2.90
S09	5407.22	12.17	14.60	2.68	0	3	0.17	0.00
S10	4520.26	14.91	14.79	0.75	5	91	5.33	1.07
S11	5346.70	13.12	13.76	1.25	16	417	24.42	1.53
S12	5361.45	13.25	15.37	2.35	7	140	8.20	1.17
S13	5399.74	18.61	15.99	2.79	5	20	1.17	0.23
S14	5380.52	15.15	14.32	1.49	16	535	31.14	1.95
S15	5315.23	16.32	14.40	1.99	12	225	13.19	1.10
S16	4287.12	14.43	14.41	0.72	6	250	14.51	2.42
Mean		**14.78**	**14.47**	**1.82**				**1.21**
STD		**1.93**	**0.60**	**0.75**				**0.74**

Movements in PLMD occur repetitive and rhythmic every 20 - 40 seconds, which generally incur a slight movement of limb or head in a short duration while sleeping. In contrast,

significant movements or position changes can take a long time. Therefore, the number of body movements every 40 seconds is counted to check the symptoms of PLMD. We also calculated the degree of body movements by dividing the movement period by the number of movements, which is assumed to be closely related to sleep quality. Figure 3.9 shows the respiratory rate and body movements of S01-S16. A blue bar represents an observed body movement. In case of observing movements several times in the beginning, it is considered that a subject had a difficulty in falling asleep, e.g. subject 04 shows the body movements at the beginning as a long time (50 minutes). Normal sleep for adults means that they fall asleep within 10 to 20 minutes after climbing into bed (sleep latency) [113]. Respiratory rates of the reference and the experiment were plotted `x' and `o', respectively. The blue column represents the histogram of body movements every 40 seconds. From this figure, we can confirm that there were no regular and repetitive body movements for all subjects during experiments, which is the typical phenomenon of PLMD.

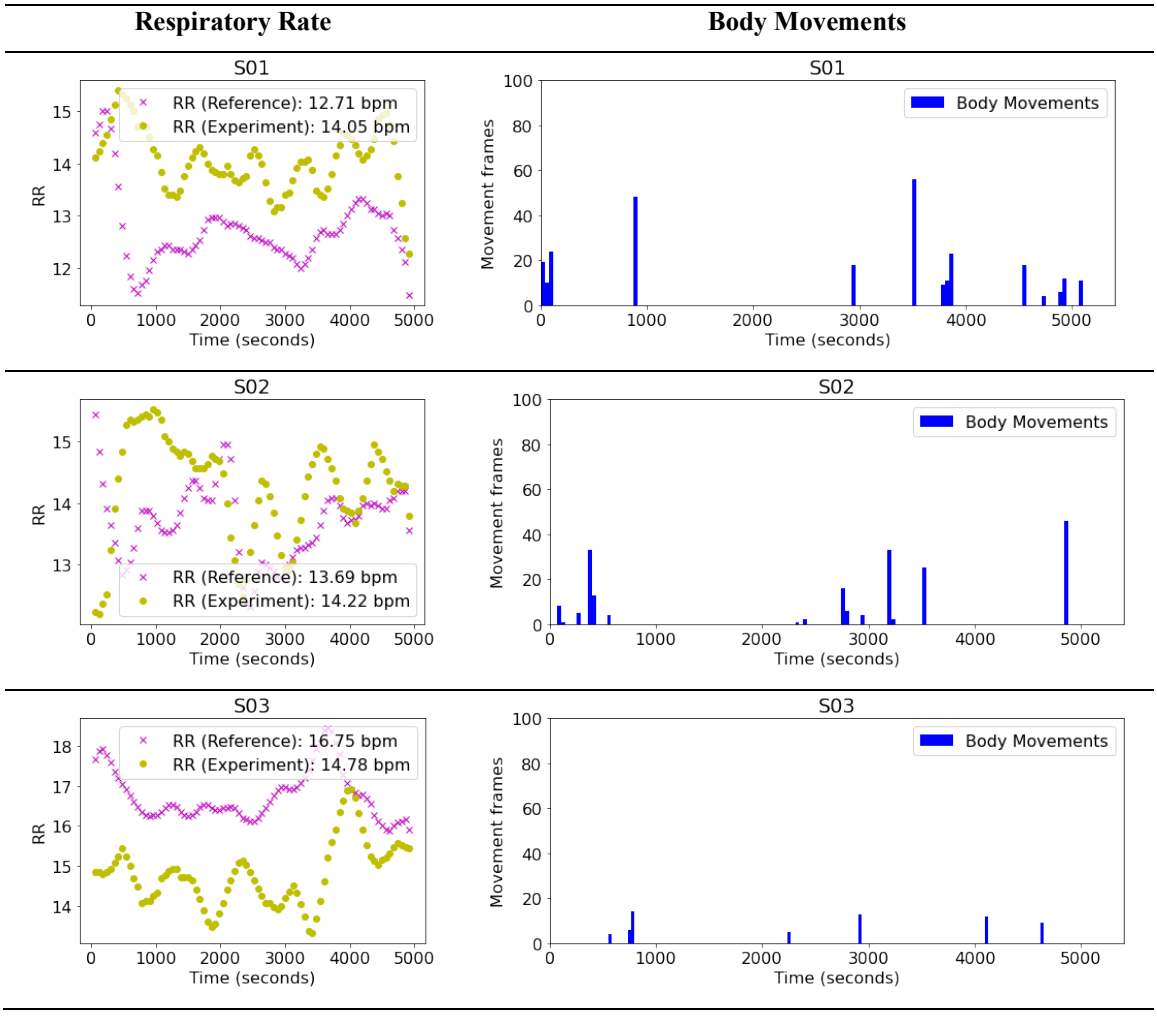

Respiratory Rate	Body Movements
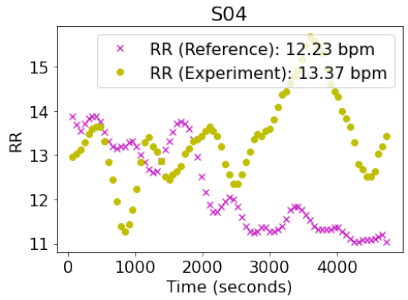	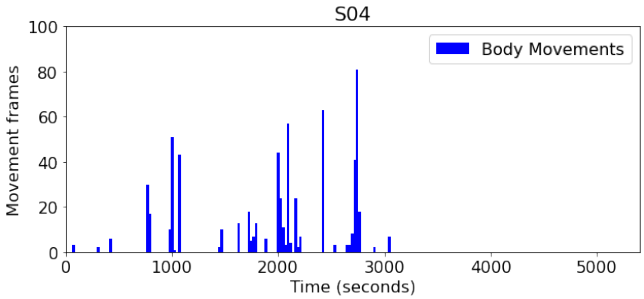
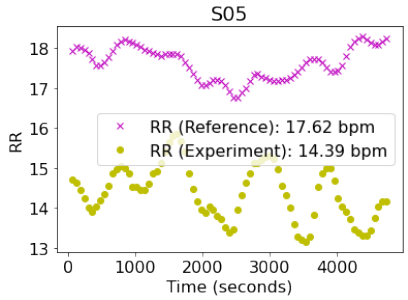	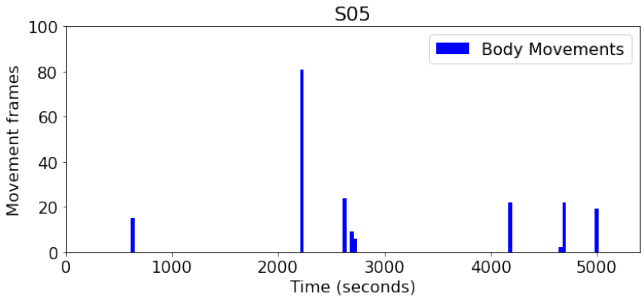
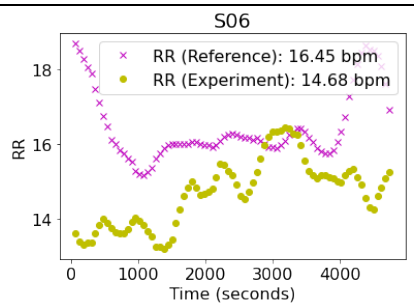	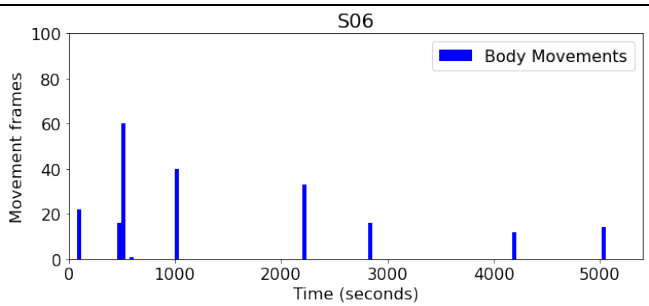
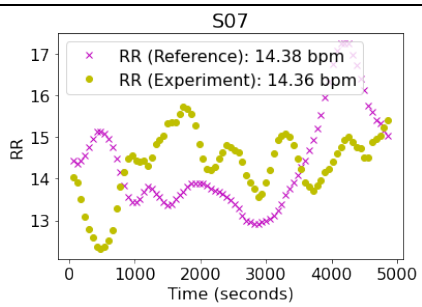	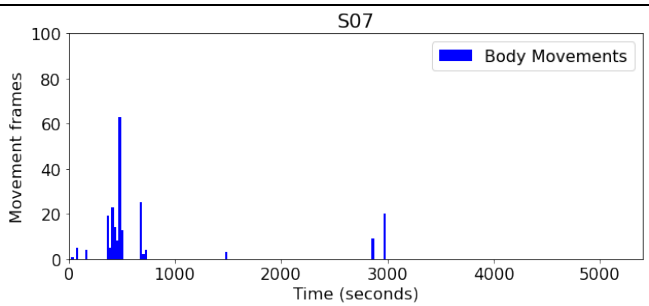
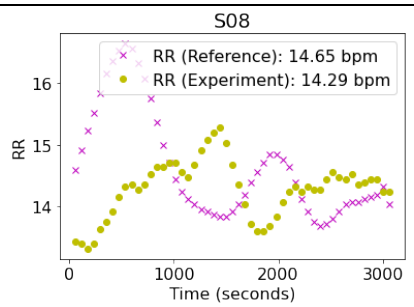	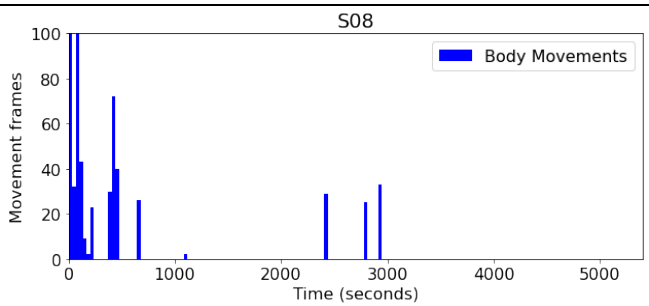

Respiratory Rate	Body Movements
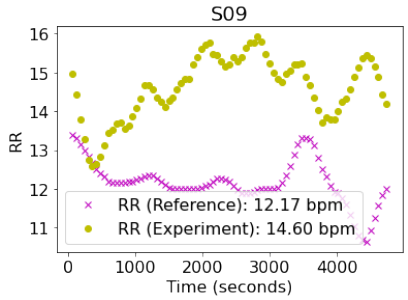	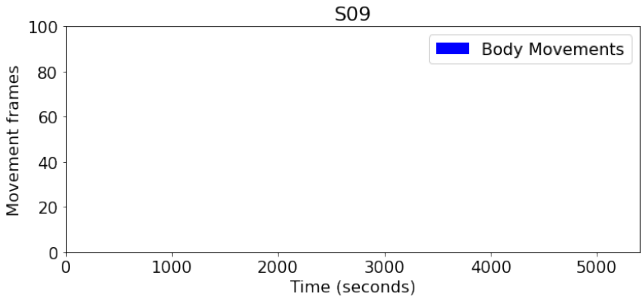
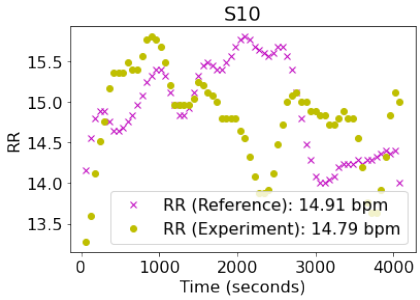	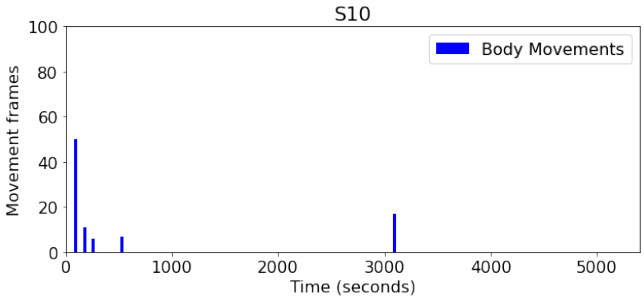
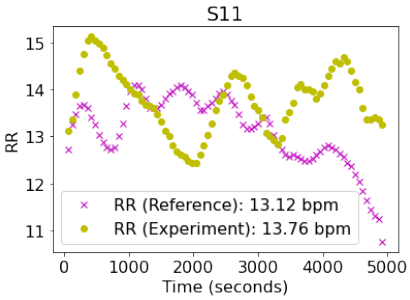	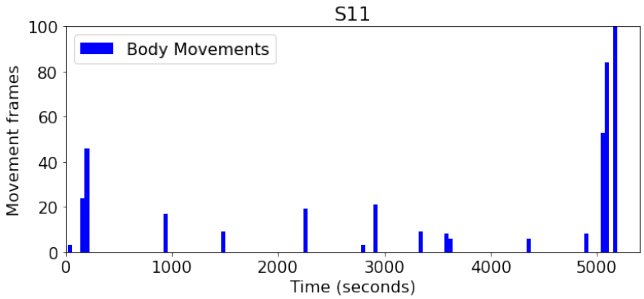
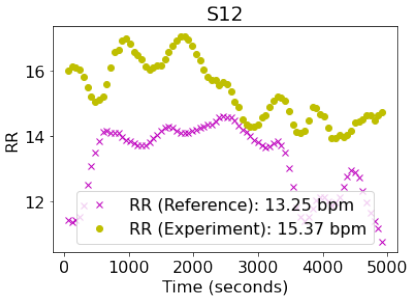	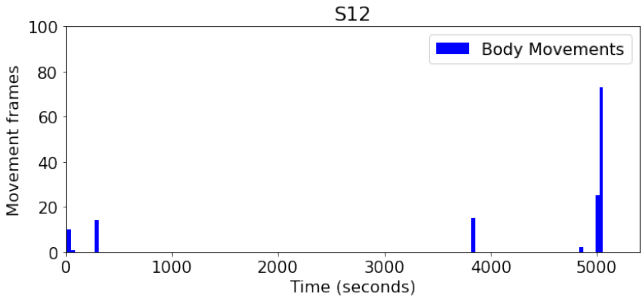
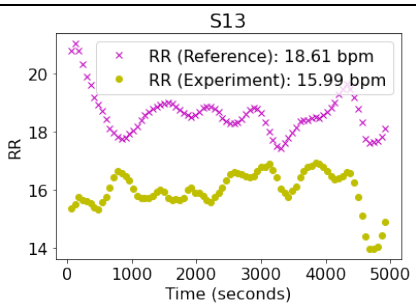	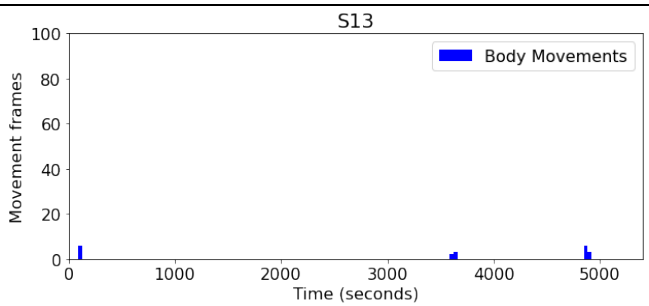

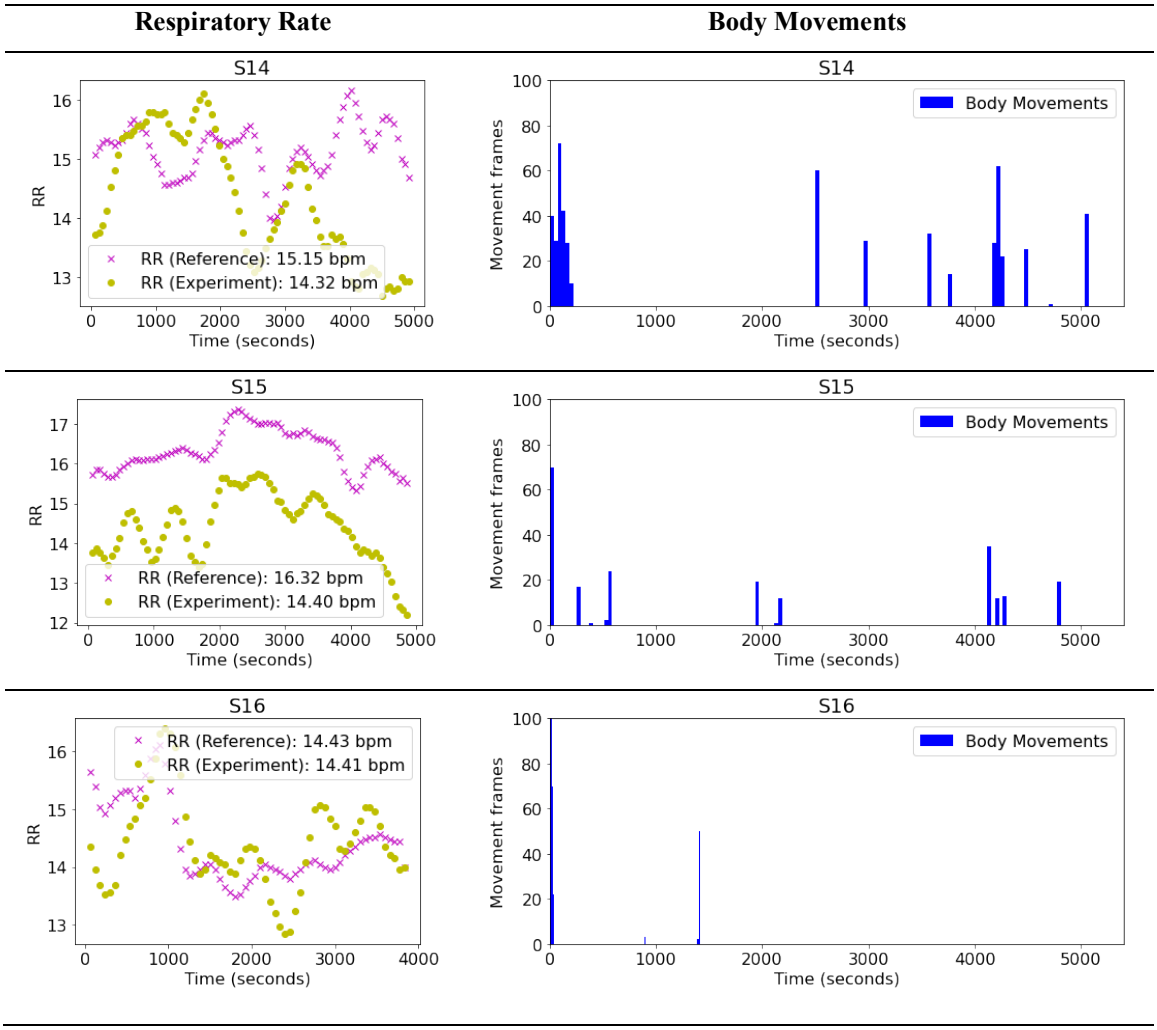

Figure 0-9: The result of respiratory rate estimation and body movements detection.

3.5 Summary

This chapter has proposed an approach for non-contact respiration monitoring and body movements detection in a natural sleep environment using a thermal camera. The thermal camera can handle many viewing angles, which enables easy installation in the bedroom. We have to overcome specific challenges to acquire non-contact respiration data from participants in their natural sleep environment when the lights were turned off, and they were covered by a blanket. Thermal video sleep monitoring can be performed in a dark environment to settle privacy concerns. The participants were asked to set up the system and perform a recording by themselves at their homes.

The proposed approach employs automatic detection of the ROIs, which is used to acquire the respiration signal and detection of the body movements of the participant based on image processing on the continuous thermal image. The signals were obtained for each frame with the process of normalization and smoothing. Then, we computed the number of breathing and counted the number of body movements. The approach has been validated using a respiratory belt as a reference signal. We evaluate respiration monitoring performance and body movements detection in different rooms with 16 participants who have independent sleep postures. Our results show that the proposed approach successfully estimated the RR with its RMSE of 1.82 ± 0.75 bpm. The performed experiments confirmed that a thermal camera is easy to use for respiration monitoring and body movements during sleeping within various environments. This study has limitations as the portable thermal camera is attached to the smartphone to record the thermal video, making the experiment duration depend on the smartphone battery.

Chapter 4
User Acceptance of Respiration Monitoring Used Thermal Camera

This chapter explores the user acceptance of the participants using a thermal camera to monitor their sleeping by themselves in their own bedroom. Here we applied a UTAUT model to measure the technology acceptance in terms of the Effort Expectancy (EE) of using a thermal camera to monitor sleep respiration. The EE is a metric for a technology that represents simpleness with reference to the needed effort for using a system.

4.1 Introduction

The use of information technology in healthcare systems has promoted healthcare quality and access to healthcare services leading to a noticeable reduction in medical errors and costs. However, attention to information technology acceptance is required when implementing any healthcare applications. There are barriers to using new technology in healthcare applications observed in human-computer interaction issues like user acceptance. The most dominant IT theories providing proper models for understanding the success and failure of IT applications appear to be Innovation Diffusion Theory (IDT) [114], Theory of Planned Behavior (TPB) [115], Model of PC Utilization (MPCU) [116], the Unified Theory of Acceptance and Use of Technology (UTAUT) [117] and the Technology Acceptance Model (TAM) [118].

TAM was designed to predict information technology acceptance and usage on the job. There are two core constructs: Perceived Usefulness (PU) and Perceived Ease of Use (PEOU). PU is

the "degree to which a person believes that using a particular system would enhance his or her job performance". On the other hand, PEOU is "the degree to which a person believes that using a particular system would be free of effort" [118], i.e., physical and mental efforts as well as ease of learning. TAM provides a direct relationship between acceptance of the technology, the technology's perceived usability, and ease of use.

Next, regarding the theories of information technology, UTAUT is widely applied model to describe the consumer acceptability of a technology. Venkatesh et al. formulated the UTAUT as shown in Figure 4.1 that proposed four behavioral intention correlations to the use of technologies [117]. First is Performance Expectancy (PE): "the degree to which an individual believes that using the system will help him or her attain gains in job performance". The second is Effort Expectancy (EE): "the degree of ease associated with the use of the system". The third correlate is Social Influence (SI): "the degree to which an individual perceives that important others believe he or she should use the new system". Finally, the fourth correlate is Facilitating Conditions (FC): "the degree to which an individual believes that an organizational and technical infrastructure exists to support the use of the system". The variables of gender, age, experience, and voluntariness of use moderate the key relationships in the model. The UTAUT model explained 69% of the intention to use IT (technology acceptance).

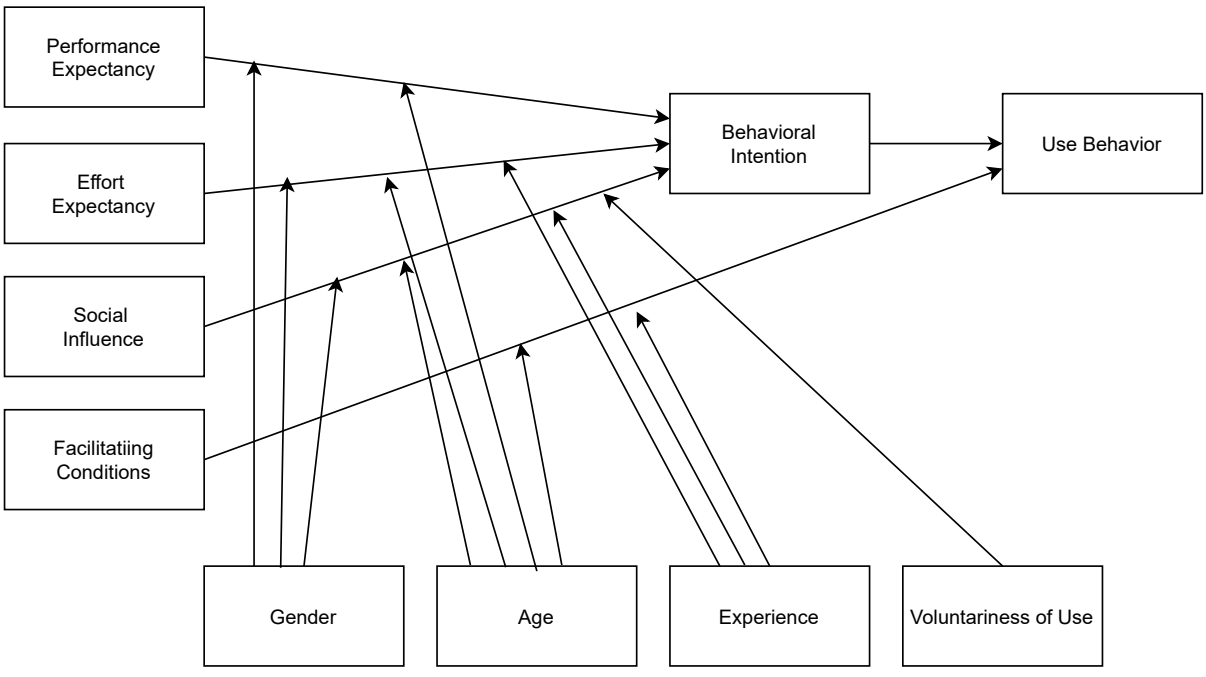

Figure 0-1: UTAUT Model [117].

Table 0.1 The ease of use definitions and scales of each model.

Constructs	Definition	Items Used in Estimation
Perceived ease of use (TAM/TAM2) [118]	The degree to which a person believes that using a particular system would be free of effort	1. Learning to operate the system would be easy for me. 2. I would find it easy to get the system to do what I want it to do. 3. My interaction with the system would be clear and understandable. 4. I would find the system to be flexible to interact with. 5. It would be easy for me to become skillful at using the system. 6. I would find the system easy to use.
Complexity (MPCU) [119]	The degree to which a system is perceived as relatively difficult to understand and use	1. Using the system takes too much time from my normal duties. 2. Working with the system is so complicated, it is difficult to understand what is going on. 3. Using the system involves too much time doing mechanical operations (e.g., data input). 4. It takes too long to learn how to use the system to make it worth the effort.
Ease of use (IDT) [120]	The degree to which using an innovation is perceived as being difficult to use	My interaction with the system is clear and understandable. I believe that it is easy to get the system to do what I want it to do. Overall, I believe that the system is easy to use. Learning to operate the system is easy for me.
Effort expectancy (UTAUT) [117]	The degree of ease associated with the use of the system	EOU3: My interaction with the system would be clear and understandable. EOU5: It would be easy for me to become skillful at using the system. EOU6: I would find the system easy to use. EU4: Learning to operate the system is easy for me.

Our study is on respiratory monitoring that combines the area of information systems, computer science, and healthcare. This system is available for patient monitoring, which can be set at home, utilizing a video camera to collect the patient's respiratory rate and body movement

during sleeping. Thus, to explore the health information technology acceptance of using the thermal camera to monitor respiration during sleeping, we consider the PU and PEOU based on the TAM and UTAUT models in health information technology acceptance of professional heath technology users. Many research has been tested in the context of healthcare [121]–[125]. Some studies found that PU and PEOU significantly impact technology adoption attitudes [124], [125]. However, the other studies found that only PU is a significant determinant of attitude and intention, but PEOU is not [121]–[123], [126]. Their results show that PU has positive effects on the usage of health information technology. Though previous studies focus on professional heath technology, the consumer health technology acceptance behavior is less discussed. Ease of use context is usually considered in the consumer health technology acceptance behavior. Therefore, we focus on the ease of use when the participants use thermal imaging to monitor their sleeping at home. Ease of use is a significant influence on the intention to use technology that constructs from the existing model as perceived ease of use (TAM/TAM2), Complexity (MPCU), and ease of use (IDT). There is a substantial similarity among constructs, definitions, and measurement scales see Table 4.1. Therefore, this study investigates the effort expectancy affecting usage behaviors using a thermal camera to monitor users during their sleep.

4.2 Data Collection

A survey was used to test the hypotheses with sixteen volunteers who used our respiratory monitoring system. We provided the devices (camera, smartphone, tripod, respiratory belt) to the volunteers to set up the system and record themselves at their homes before going to bed. It can handle many viewing angles, which makes installation in the bedroom easy. The thermal camera is used to obtain respiratory information and body movements in natural sleep environments such as a dark room to settle privacy concerns. Since the users closed the lighting, the acquired video images differed in their overall brightness. Nevertheless, the video recording process is carried out with the same settings following the instruction.

The scaled items for effort expectancy were adapted from the UTAUT model shown in Table 4.2. The scales are slightly modified to suit the context of the use of the thermal camera. Each item is measured using a five-point Likert-type scale, ranging from “strongly disagree” (1) to “strongly agree” (5). Demographic data about gender and age were collected to describe the

sample characteristics. Data were collected using an online survey method developed by Google Form.

Table 0.2 Scale items for estimate the effort expectancy.

Items	SA (5)	A (4)	US (3)	DA (2)	SDA (1)
Learning how to use a thermal camera is easy for me.					
My interaction with the thermal camera is clear and understandable.					
I find the thermal camera easy to use.					
It is easy for me to become skillful at using a thermal camera.					

4.3 Results

All 16 completed questionnaires are returned, i.e. 100% response rate. The detailed sample characteristics are described in Table 4.3.

Table 0.3 Descriptive statistics of respondents' characteristics.

Measurement	Items	Frequency	%
Gender	Female	10	62.50
	Male	6	37.50
Age	$\geq 25 < 30$ years	9	56.25
	$\geq 30 < 35$ yesrs	5	31.25
	≥ 35 years	2	12.50

Table 0.4 Effort Expectancy of Using Thermal Camera to Monitor Sleeping.

Items	Response (%)						
	SA	A	US	DA	SDA	Mean	SD
EE1	56.25	25.00	18.75	0.00	0.00	4.38	0.19
EE2	37.50	43.75	18.75	0.00	0.00	4.19	0.15
EE3	56.25	31.25	12.50	0.00	0.00	4.44	0.19
EE4	43.75	37.50	18.75	0.00	0.00	4.25	0.15
Overall	**48.44**	**34.38**	**17.19**	**0.00**	**0.00**	**4.38**	**0.19**

Note: SA = Strongly Agreed (5), A = Agreed (4), S = Unsure (3), DA = Disagreed (2), SDA= Strongly Disagreed (1), M = Mean, SD = Standard Deviation

Table 4.4 shows participants' responses for items associated with their levels of satisfaction with using the thermal video to monitor sleeping. The results show that 82.81% of the

participants were satisfied with using the thermal camera in this monitoring (mean = 4.38; standard deviation, SD = 0.22). It is clarified that the use of thermal video to monitor sleeping promises it's easy to use.

4.4 Conclusion

This study concerns the consumer of health technology acceptance behavior in using the thermal camera for monitoring respiratory while sleeping at home. This system is useful for the consumer by providing potential prediction and risk reduction of serious illness. Nowadays, the respiratory monitoring system was developed through video monitoring without any device attached to the body, while privacy is an important issue, especially in the sleep environment. The respiratory monitoring system offers valuable functionalities. To improve the practicability of the respiratory monitoring system, the system must be developed by considering users' actual needs, technology adoption, convenience, etc. Thus, an acceptance of the respiratory monitoring system from the users' perspective should be necessarily evaluated. Therefore, we estimated the ease of use from users' perspective by measuring the effort expectancy based on the UTAUT model, which indicates the intention to use. The result shows that the participants are satisfied with using the thermal camera to monitor their respiratory while sleeping at home.

Chapter 5
Conclusion

In this dissertation, non-contact respiratory monitoring in sleeping posture using a smartphone camera and thermal camera has been introduced. The goals are (i) to determine the accuracy of respiratory rate estimation by comparing with ground truth data, (ii) to identify the factors that influence respiratory information extraction, (iii) to provide the prototype development of the non-contact system, and (iv) to discuss the factors that affect the health information technology acceptance. The content goes from the respiratory monitoring in sleep position using a smartphone camera to capture the high frame rate video and the ordinary video, through the using the thermal camera to capture in the natural sleep environment and ends at the estimation of use acceptance when using the thermal camera for monitoring their respiratory in the actual situation.

5.1 Conclusion

Chapter 2 discussed the use of a smartphone camera at a high frame rate to record video in a sleeping position, which is the beginning of the research study. The environment is set in the visible room for this experiment, and the blanket does not cover the subjects. The smartphone camera is set on the tripod to capture breath movement around the waist and shoulder area of the subjects in a lie on the side of sleeping positions at a 240 fps of frame rate. There are two issues to estimate the respiratory in the sleeping position. The first issue is the ROI selection which is significantly related to the respiratory. The ROI with its size of 50 x50 pixels is placed around the waist or shoulder of the subjects that also contain a background view to observe the body movement. Then used the Gaussian blur filter to reduce the noise within that ROI. Besides, the MOSSE tracker has been applied to track the selected ROI movement.

The second issue is the respiratory signal extraction that is calculated from the intensity value within the ROI of each frame. When obtaining the signal, the Butterworth with a low pass and Filtfilt filter was applied to. The Fast Fourier Transform was used to find the suitable window length to the Savitzky-Golay filter. The last step was to use the Findpeaks function to count the number of breaths. The results demonstrated the high accuracy of respiratory estimation and confirmed that the accuracy depends on the location and size of the ROI. In other words, the region of interest location is a significant point to detect breathing movement. Moreover, the background view affects the accuracy of the breathing rate estimation. The white and no pattern of background is recommended in this study.

Regarding the effect from the background view and the clothing pattern, we experimented again with the ordinary video at 30 fps. We used a black blanket to cover the subject and set the experiment in a room with no background pattern. In the second experiment, we proposed an automatic ROI selection to measure the respiratory rate and its patterns using the ordinary video. This study demonstrated that the respiratory rate could be assessed successfully using a smartphone camera to capture the chest or abdomen's breathing movement under a blanket in lying on the back and lying on the side positions. Our automatic ROI selection method uses motion detection based on the differences between two frames to detect the respiratory movement in the video. We used the average of the pixels in the region to estimate the respiratory rate and its patterns. The experimental results showed that the respiratory rates were successfully measured at different sleeping positions, with its RMSE of 0.47 (lying on the back), 1.60 (lying on the side), and 1.18 as an average. Under a controlled environment, linear regression analysis showed that the measured respiratory signal had a relatively good relationship with a ground truth signal, with a determination coefficient of 0.914. The suggestion is that the small region provides the most accurate respiratory rate estimation among camera-based approaches. This work's limitation is noise caused by lip-smacking, eye movement, and body movement while sleeping. These are uncontrolled movements would be detected by the difference between frames, which degraded the performance. In the future, we will extend our automatic ROI selection to comply with a variety of sleeping positions with properly updating the ROI location.

In Chapter 3, we coordinated the experiment based on thermal video with the blanket in real-life conditions, implying an uncontrolled sleep posture, darkness, and subjects covered with a blanket. The automatic ROI extraction by temperature detection and breathing motion

detection based on image processing are integrated to obtain the respiration signals. A signal processing technique was used to estimate respiration and body movement information from a sequence of thermal videos. The proposed approach has been tested on 16 volunteers, for which video recordings were carried out by themselves. The participants were also asked to wear the Go Direct respiratory belt for capturing reference data. The result revealed that our proposed respiratory estimation system obtains RMSE of 1.82 ± 0.75 bpm.

Chapter 4 tested the user technology acceptance from the user's perspective when using the thermal camera to monitor the respiratory during sleeping at home. The effort expectancy was evaluated based on the UTAUT model by participants who participated in the experiment in chapter 3. The result shows that they were satisfied with the ease of using our proposed system.

This dissertation has studied the non-contact respiratory monitoring in the sleeping position using cameras. The challenge is automatic to specify the region of interest in sleeping positions in uncontrolled posture while sleeping. The study starts with the fundamental of the conventional approach to image processing and proposed solutions. Next, the non-contact respiratory and sleep monitoring in the actual environment has been addressed by using the thermal camera. However, because the participants in the study did not have respiratory problems, only the respiratory estimation accuracy can be provided based on ROI detection. In future work, we will focus on monitoring a patient who has irregular breathing. Another element of our future work is continuing to develop the automatic optimization of the thresholding value. The other limitations of the proposed method, such as a variation of room temperature, the type of bed cover, blanket, and night sweats (neck or face) in subjects, rapid eye movement (REM) stage, and heart rate, provide ideas for addressing these issues in future studies.

5.2 Future Work

The proposed approach to monitoring respiration in sleeping positions is carried out in several test scenarios to test the system's reliability in measuring RR, for example, using various kinds of bed covers or blankets. Thermal video can be performed in a dark environment to settle privacy concerns. Moreover, using thermal cameras is a part of non-contact monitoring to support current telemedicine technology and provides a hygienic aspect for users in the COVID-19 pandemic. There are no components attached to the body to minimize contact

between users. Therefore, the results obtained through the course of this research should be viable for practical use, especially in the post-pandemic era.

However, the participants in this study are healthy; therefore, no exploration with the person who has an abnormal respiratory. We will explore experimenting with applying the thermal camera to patients with broader subject demographics who have respiration conditions as a disorder for future work.

There also remains a room for developing more sophisticated algorithms to raise the detection quality. The future algorithm should be able to distinguish apneas from gross body motion, usable during day and nighttime, independent of skin visibility and body tracking.

Because the video duration has been recorded at approximately 1.30 hours depending on the smartphone's battery life when using the smartphone's portable thermal camera, the whole night monitoring using a thermal camera will also be examined in the future.

Furthermore, the automatic determination and adjustment of the threshold value used to detect the observed area and motion detection are to be considered. Classification of movements as breath movements or body movements may contribute to raising detection performance.

References

[1] M. Cretikos, J. Chen, K. Hillman, R. Bellomo, S. Finfer, and A. Flabouris, "The objective medical emergency team activation criteria: A case–control study," Resuscitation, vol. 73, no. 1, pp. 62-72, 2007.

[2] K. Zhu, M. Li, S. Akbarian, M. Hafezi, A. Yadollahi, and B. Taati, "Vision-based heart and respiratory rate monitoring during sleep - A validation study for the population at risk of sleep apnea," IEEE J. Transl. Eng. Health Med., vol. 7, p. 1900708, 2019.

[3] T. J. Hodgetts, G. Kenward, I. G. Vlachonikolis, S. Payne, and N. Castle, "The identification of risk factors for cardiac arrest and formulation of activation criteria to alert a medical emergency team," *Resuscitation*, vol. 54, no. 2, pp. 125-131, 2002.

[4] R. Maharaj, I. Raffaele, and J. Wendon, "Rapid response systems: a systematic review and meta-analysis," *Crit. Care*, vol. 19, no. 1, p. 254, 2015.

[5] P. P. Ponikowski, T. P. Chua, D. P. Francis, A. Capucci, A. J. S. Coats, and M. F. Piepoli, "Muscle Ergoreceptor Overactivity Reflects Deterioration in Clinical Status and Cardiorespiratory Reflex Control in Chronic Heart Failure," *Circulation*, vol. 104, no. 19, pp. 2324-2330, 2001.

[6] C. Rambaud-Althaus, F. Althaus, B. Genton, and V. D'Acremont, "Clinical features for diagnosis of pneumonia in children younger than 5 years: a systematic review and meta-analysis," *Lancet Infect. Dis.*, vol. 15, no. 4, Apr. 2015.

[7] P. Egermayer, G. I. Town, J. G. Turner, D. C. Heaton, A. L. Mee, and M. E. J. Beard, "Usefulness of D-dimer, blood gas, and respiratory rate measurements for excluding pulmonary embolism," *Thorax*, vol. 53, no. 10, Oct. 1998.

[8] C. Galle, J. P. Papazyan, M. J. Miron, D. Slosman, H. Bounameaux, and A. Perrier, "Prediction of pulmonary embolism extent by clinical findings, D-dimer level and deep vein thrombosis shown by ultrasound," *Thromb. Haemost.*, vol. 86, no. 5, 2001.

[9] M. J. Tobin, F. Laghi, and L. Brochard, "Role of the respiratory muscles in acute respiratory failure of COPD: lessons from weaning failure," *J. Appl. Physiol.*, vol. 107, no. 3, Sep. 2009.

[10] N. Hochhausen, C. B. Pereira, S. Leonhardt, R. Rossaint, and M. Czaplik, "Estimating respiratory rate in post-anesthesia care unit patients using infrared thermography: An observational study," *Sensors,* vol. 18, no. 5, May 2018.

[11] Y. Matsuura, H. Jeong, K. Yamada, K. Watabe, K. Yoshimoto, and Y. Ohno, "Screening Sleep Disordered Breathing with Noncontact Measurement Screening Sleep Disordered

Breathing with Noncontact Measurement in a Clinical Site." *Journal of Robotics and Mechatronics*, *29*(2), 327-337.

[12] J.-C. Cobos-Torres, M. Abderrahim, and J. Martínez-Orgado, "Non-Contact, Simple Neonatal Monitoring by Photoplethysmography," *Sensors*, vol. 18, no. 12, Dec. 2018.

[13] M. Villarroel1, J. Jorge1, C. Pugh, L. Tarassenko "Non-contact vital sign monitoring in the clinic," in *2017 12th IEEE International Conference and Workshops on Automatic Face and Gesture Recognition (FG2017)*, pp. 278-825, 2017.

[14] L. Tarassenko, M. Villarroel, A. Guazzi, J. Jorge, D. A. Clifton, and C. Pugh, "Non-contact video-based vital sign monitoring using ambient light and auto-regressive models," *Physiol. Meas.*, vol. 35, no. 5, pp. 807–831, May 2014.

[15] M. Hu *et al.*, "Combination of near-infrared and thermal imaging techniques for the remote and simultaneous measurements of breathing and heart rates under sleep situation," *PLoS One*, vol. 13, no. 1, Jan. 2018.

[16] S. Kang *et al.*, "Non-contact diagnosis of obstructive sleep apnea using impulse-radio ultra-wideband radar," *Sci. Rep.*, vol. 10, no. 1, Dec. 2020.

[17] K. Nakajima, Y. Matsumoto, and T. Tamura, "A monitor for posture changes and respiration in bed using real time image sequence analysis," *Annu. Int. Conf. IEEE Eng. Med. Biol. - Proc.*, vol. 1, pp. 51–54, 2000.

[18] M. Frigola, J. Amat, and J. Pagès, " Vision based respiratory monitoring system." in *Proceedings of the 10th Mediterranean Conference on Control and Automation (MED 2002), Lisbon, Portugal,* pp. 9-13, July, 2012.

[19] K. Zhu, M. Li, S. Akbarian, M. Hafezi, A. Yadollahi, and B. Taati, "Vision-Based Heart and Respiratory Rate Monitoring during Sleep-A Validation Study for the Population at Risk of Sleep Apnea," *IEEE J. Transl. Eng. Heal. Med.*, vol. 7, 2019.

[20] I. Sato and M. Nakajima, "Non-contact Breath Motion Monitor ing System in Full Automation," in *2005 IEEE Engineering in Medicine and Biology 27th Annual Conference,* pp. 3448-3451, January, 2005.

[21] C. W. Wang, A. Ahmed, and A. Hunter, "Vision analysis in detecting abnormal breathing activity in application to diagnosis of obstructive sleep apnoea.," *Conf. Proc. IEEE Eng. Med. Biol. Soc.*, pp. 4469–4473, 2006.

[22] R. Janssen, W. Wang, A. Moço, and G. De Haan, "Video-based respiration monitoring with automatic region of interest detection," *Physiol. Meas.*, 2015.

[23] C. W. Wang, A. Hunter, N. Gravill, and S. Matusiewicz, "Real time pose recognition of covered human for diagnosis of sleep apnoea," *Comput. Med. Imaging Graph.*, vol. 34, no. 6, pp. 523–533, Sep. 2010.

[24] C. W. Wang, A. Hunter, N. Gravill, and S. Matusiewicz, "Unconstrained video monitoring of breathing behavior and application to diagnosis of sleep apnea," *IEEE Trans. Biomed. Eng.*, vol. 61, no. 2, pp. 396–404, Feb. 2014.

[25] L. Ren, H. Wang, K. Naishadham, Q. Liu, and A. E. Fathy, "Non-invasive detection of cardiac and respiratory rates from stepped frequency continuous wave radar measurements using the state space method," in *2015 IEEE MTT-S International Microwave Symposium, IMS2015*, pp. 1-4, 2015.

[26] A. Al-Naji and J. Chahl, "Remote respiratory monitoring system based on developing motion magnification technique," *Biomed. Signal Process. Control*, vol. 29, pp. 1–10, 2016.

[27] I. Lorato, S. Stuijk, M. Meftah, W. Verkruijsse, and G. De Haan, "Camera-based On-line Short Cessation of Breathing Detection."

[28] M. Bartula, T. Tigges, and J. Muehlsteff, "Camera-based system for contactless monitoring of respiration," in *Proceedings of the Annual International Conference of the IEEE Engineering in Medicine and Biology Society, EMBS*, pp. 2672-2675, July, 2013.

[29] N. Koolen, O. Decroupet, A. Dereymaeker, K.Jansen, J. Vervisch, V. Matic,…, & M. De Vos, "Automated Respiration Detection from Neonatal Video Data." *ICPRAM (2),* pp. 164-169, January, 2015.

[30] M. Hu *et al.*, "Combination of near-infrared and thermal imaging techniques for the remote and simultaneous measurements of breathing and heart rates under sleep situation," *PLoS One*, vol. 13, no. 1, Jan. 2018.

[31] G. Yuan, N. A. Drost, and R. A. McIvor, "Respiratory rate and breathing pattern," *McMaster Univ. Med. J.*, vol. 10, no. 1, pp. 23–25, 2013.

[32] B. Bozkurt and D. L. Mann, "Cardiology patient page. Shortness of Breath," *Circulation*, vol. 108, no. 2, pp. e11-3, 2003.

[33] D. R. Goldhill, A. F. McNarry, G. Mandersloot, and A. McGinley, "A physiologically-based early warning score for ward patients: the association between score and outcome," *Anaesthesia*, vol. 60, no. 6, 2005.

[34] J. Kellett, M. Li, S. Rasool, G. C. Green, and A. Seely, "Comparison of the heart and breathing rate of acutely ill medical patients recorded by nursing staff with those measured over 5min by a piezoelectric belt and ECG monitor at the time of admission to hospital," *Resuscitation*, vol. 82, no. 11, Nov. 2011.

[35] T. Flenady, T. Dwyer, and J. Applegarth, "Accurate respiratory rates count: So should you!," *Australas. Emerg. Nurs. J.*, vol. 20, no. 1, Feb. 2017.

[36] C. Massaroni, A. Nicolò, D. Lo Presti, M. Sacchetti, S. Silvestri, and E. Schena, "Contact-based methods for measuring respiratory rate," *Sensors*, vol. 19, no. 4. MDPI AG, 02-Feb-2019.

[37] A. H. Alkali, R. Saatchi, H. Elphick, and D. Burke, "Thermal image processing for real-time non-contact respiration rate monitoring," *IET Circuits, Devices Syst.*, vol. 11, no. 2, pp. 142–148, Jul. 2017.

[38] E. A. Bernal, L. K. Mestha, and E. Shilla, "Non contact monitoring of respiratory

function via depth sensing," *IEEE-EMBS International Conference on Biomedical and Health Informatics*, 2014, pp.101-104.

[39] M. Martinez and R. Stiefelhagen, "Breath rate monitoring during sleep using near-ir imagery and PCA," *Proceedings of the 21st International Conference on Pattern Recognition (ICPR2012)*, 2012, pp. 3472–3475.

[40] T. Lukac, J. Pucik, and L. Chrenko, "Contactless recognition of respiration phases using web camera," *2014 24th International Conference Radioelektronika*, 2014, pp. 1-4.

[41] C. Massaroni, A. Nicolo, M. Sacchetti, and E. Schena, "Contactless Methods For Measuring Respiratory Rate: A Review," in *IEEE Sensors Journal*, vol.21, no. 11, pp. 12821–12829, 2021.

[42] J. Liu, Y. Chen, Y. Wang, X. Chen, J. Cheng, and J. Yang, "Monitoring Vital Signs and Postures during Sleep Using WiFi Signals," in *IEEE Internet Things J.*, vol. 5, no. 3, pp. 2071–2084, June, 2018.

[43] F. Lin *et al.*, "SleepSense: A Noncontact and Cost-Effective Sleep Monitoring System," *IEEE Trans. Biomed. Circuits Syst.*, vol. 11, no. 1, Feb. 2017.

[44] Y. Gu, X. Zhang, Z. Liu, and F. Ren, "WiFi-Based Real-Time Breathing and Heart Rate Monitoring during Sleep," in *2019 IEEE Global Communications Conference (GLOBECOM)*, 2019.

[45] M. Zakrzewski, A. Vehkaoja, A. S. Joutsen, K. T. Palovuori, and J. J. Vanhala, "[]," *IEEE Sens. J.*, vol. 15, no. 10, Oct. 2015.

[46] E. E. Geertsema, G. H. Visser, J. W. Sander, and S. N. Kalitzin, "Automated non-contact detection of central apneas using video," *Biomed. Signal Process. Control*, vol. 55, Jan. 2020.

[47] K. Zhu, M. Li, S. Akbarian, M. Hafezi, A. Yadollahi, and B. Taati, "Vision-Based Heart and Respiratory Rate Monitoring during Sleep-A Validation Study for the Population at Risk of Sleep Apnea," *IEEE J. Transl. Eng. Heal. Med.*, vol. 7, 2019.

[48] F. Deng *et al.*, "Design and Implementation of a Noncontact Sleep Monitoring System Using Infrared Cameras and Motion Sensor," *IEEE Trans. Instrum. Meas.*, vol. 67, no. 7, Jul. 2018.

[49] M. H. Li, A. Yadollahi, and B. Taati, "Noncontact Vision-Based Cardiopulmonary Monitoring in Different Sleeping Positions," *IEEE J. Biomed. Heal. Informatics*, 2017.

[50] M. H. Li, A. Yadollahi, and B. Taati, "A non-contact vision-based system for respiratory rate estimation," in *2014 36th Annual International Conference of the IEEE Engineering in Medicine and Biology Society, EMBC 2014*, 2014, pp. 2119–2122.

[51] A. K. Abbas, K. Heimann, K. Jergus, T. Orlikowsky, and S. Leonhardt, "Neonatal non-contact respiratory monitoring based on real-time infrared thermography," *Biomed. Eng. Online*, 2011.

[52] Usman and R. Muhammad, "Non-invasive respiration monitoring by thermal imaging

to detect sleep apnoea." *The 32nd International Congress and Exhibition on Condition Monitoring and Diagnostic Engineering Management*, Huddersfield, 3 Sep 2019 - 5 Sep 2019. (Unpublished)

[53] L. Walsh and S. McLoone, "Non-contact under-mattress sleep monitoring," *J. Ambient Intell. Smart Environ.*, vol. 6, no. 4, 2014.

[54] K. Nakajima, Y. Matsumoto, and T. Tamura, "Development of real-time image sequence analysis for evaluating posture change and respiratory rate of a subject in bed," in *Physiological Measurement*, 2001, vol. 22, no. 3, p. 21.

[55] Y. Takemura, J. Y. Sato, and M. Nakajima, "A respiratory movement monitoring system using fiber-grating vision sensor for diagnosing sleep apnea syndrome," *Opt. Rev.*, vol. 12, no. 1, pp. 46–53, Jan. 2005.

[56] S. Wiesner and Z. Yaniv, "Monitoring patient respiration using a single optical camera," in *2007 29th Annual International Conference of the IEEE Engineering in Medicine and Biology*, 2007, pp. 2740–2743.

[57] F. Zhao, M. Li, Y. Qian, and J. Z. Tsien, "Remote Measurements of Heart and Respiration Rates for Telemedicine," *PLoS One*, 2013.

[58] V. V. Makkapati and S. S. Rambhatla, "Camera based estimation of respiration rate by analyzing shape and size variation of structured light," in *2016 IEEE International Conference on Acoustics, Speech and Signal Processing (ICASSP)*, 2016, pp 2219-2223.

[59] K. Y. Lin, D. Y. Chen, and W. J. Tsai, "Image-Based Motion-Tolerant Remote Respiratory Rate Evaluation," *IEEE Sensors Journal*, *16*(9), 3263-3271, 2016.

[60] B. Wei, X. He, C. Zhang, and X. Wu, "Non-contact, synchronous dynamic measurement of respiratory rate and heart rate based on dual sensitive regions," *Biomed. Eng. Online*, vol. 16, no. 1, Jan. 2017.

[61] C. Wiede, J. Richter, M. Manuel, and G. Hirtz, "Remote Respiration Rate Determination in Video Data - Vital Parameter Extraction based on Optical Flow and Principal Component Analysis," in *12th International Joint Conference on Computer Vision, Imaging and Computer Graphics Theory and Applications*, Vol. 5, pp. 326-333. SCITEPRESS, February, 2017.

[62] C. Massaroni, E. Schena, S. Silvestri, F. Taffoni, and M. Merone, "Measurement system based on RBG camera signal for contactless breathing pattern and respiratory rate monitoring," in *2018 IEEE International Symposium on Medical Measurements and Applications(MeMeA),* pp. 1-6, 2018.

[63] D. Shao, Y. Yang, C. Liu, F. Tsow, H. Yu, and N. Tao, "Noncontact monitoring breathing pattern, exhalation flow rate and pulse transit time," *IEEE Trans. Biomed. Eng.*, 2014.

[64] H. Y. Wu, M. Rubinstein, E. Shih, J. Guttag, F. Durand, and W. Freeman, "Eulerian video magnification for revealing subtle changes in the world," *ACM Trans. Graph.*, vol. 31, no. 4, 2012.

[65] K. S. Tan, R. Saatchi, H. Elphick, "Real-Time Vision Based Respiration Monitoring System. " in *2010 7th International Symposium on Communication Systems, Networks & Digital Signal Processing (CSNDSP 2010),* 2010, pp. 770-774.

[66] R. Janssen, W. Wang, A. Moço, and G. De Haan, "Video-based respiration monitoring with automatic region of interest detection," *Physiol. Meas.*, 2015.

[67] D. Alinovi, G. Ferrari, F. Pisani, and R. Raheli, "Respiratory rate monitoring by maximum likelihood video processing," in *2016 IEEE International Symposium on Signal Processing and Information Technology, ISSPIT 2016*, 2017, pp. 172–177.

[68] Harvard Medical School, "Understanding the Results - Sleep Apnea," *Harvard Medical School - Division of Sleep Medicine*, 2011. [Online]. Available: http://healthysleep.med.harvard.edu/sleep-apnea/diagnosing-osa/understanding-results. [Accessed: 09-Dec-2019].

[69] D. Shao, Y. Yang, C. Liu, F. Tsow, H. Yu, and N. Tao, "Noncontact monitoring breathing pattern, exhalation flow rate and pulse transit time," *IEEE Trans. Biomed. Eng.*, vol. 61, no. 11, pp. 2760–2767, 2014.

[70] E. Schena, D. S. Lopes, D. Lo Presti, S. Silvestri, and C. Massaroni, "Contactless Monitoring of Breathing Patterns and Respiratory Rate at the Pit of the Neck: A Single Camera Approach," *J. Sensors*, vol. 2018, pp. 1–13, 2018.

[71] Y. W. Bai, W. T. Li, and Y. W. Chen, "Design and implementation of an embedded monitor system for detection of a patient's breath by double webcams," in *2010 IEEE International Workshop on Medical Measurements and Applications,* 2010, pp. 171–176.

[72] M. Z. Poh, D. J. McDuff, and R. W. Picard, "Advancements in noncontact, multiparameter physiological measurements using a webcam," *IEEE Trans. Biomed. Eng.*, vol. 58, no. 1, pp. 7–11, 2011.

[73] B. A. Reyes, N. Reljin, Y. Kong, Y. Nam, and K. H. Chon, "Tidal Volume and Instantaneous Respiration Rate Estimation using a Volumetric Surrogate Signal Acquired via a Smartphone Camera," *IEEE J. Biomed. Heal. Informatics*, vol. 21, no. 3, 2017.

[74] M. D. Buist, E. Jarmolowski, P. R. Burton, S. A. Bernard, B. P. Waxman, and J. Anderson, "Recognising clinical instability in hospital patients before cardiac arrest or unplanned admission to intensive care. A pilot study in a tertiary-care hospital," *Med. J. Aust.*, vol. 171, no. 1, 1999.

[75] C. Franklin and J. Mathew, "Developing strategies to prevent inhospital cardiac arrest: Analyzing responses of physicians and nurses in the hours before the event," *Crit. Care Med.*, vol. 22, no. 2, 1994.

[76] Y. Nam, Y. Kong, B. Reyes, N. Reljin, and K. H. Chon, "Monitoring of heart and breathing rates using dual cameras on a smartphone," *PLoS One*, 2016.

[77] David S. Bolme J. Ross Beveridge Bruce A. Draper Yui Man Lui, "Visual

Object Tracking using Adaptive Correlation Filters," *2010 IEEE computer society conference on computer vision and pattern recognition,* 2010, pp. 2544-2550

[78] A. Savitzky and M. J. Goley, "Smoothing and Differentiation of Data by Simplified Least Squares Procedures," *Analytical chemistry*, vol. 36, no. 8, pp. 1627–1639, 1964.

[79] A. Savitzky and M. J. Goley, "Smoothing and Differentiation of Data by Simplified Least Squares Procedures," *Analytical chemistry*, vol. 36, no. 8, pp. 1627–1639, 1964.

[80] Z. Wang, A. C. Bovik, H. R. Sheikh, and E. P. Simoncelli, "Image quality assessment: From error visibility to structural similarity," *IEEE Trans. Image Process.*, vol. 13, no. 4, 2004.

[81] I. W. Selesnick and C. Sidney Burrus, "Generalized digital butterworth filter design," *IEEE Trans. Signal Process.*, vol. 46, no. 6, 1998.

[82] W. H. Press and S. A. Teukolsky, "Savitzky-Golay Smoothing Filters," *Comput. Phys.*, vol. 4, no. 6, 1990.

[83] A. L. Meoli *et al.*, "Hypopnea in sleep-disordered breathing in adults.," *Sleep*, vol. 24, no. 4, pp. 469–70, 2001.

[84] M. A. E. Zagaria, "Periodic limb movement disorder, restless legs syndrome, and pain," *U.S. Pharm.*, vol. 40, no. 3, 2015.

[85] P. Madhushri, B. Ahmed, T. Penzel, and E. Jovanov, "Periodic leg movement (PLM) monitoring using a distributed body sensor network," in *2015 37th Annual International Conference of the IEEE Engineering in Medicine and Biology Society, EMBS*, pp. 1837-1840, August, 2015.

[86] A. Kwasniewska, J. Ruminski, and M. Szankin, "Improving accuracy of contactless respiratory rate estimation by enhancing thermal sequences with deep neural networks," *Appl. Sci.*, vol. 9, no. 20, Oct. 2019.

[87] A. K. Abbas, K. Heiman, T. Orlikowsky, and S. Leonhardt, "Non-Contact Respiratory Monitoring Based on Real-Time IR-Thermography," in *World Congress on Medical Physics and Biomedical Engineering, September 7 - 12, 2009, Munich, Germany*, 2010, pp. 1306–1309.

[88] F. Q. Al-Khalidi, R. Saatchi, D. Burke, and H. Elphick, "Tracking human face features in thermal images for respiration monitoring," in *2010 ACS/IEEE International Conference on Computer Systems and Applications, AICCSA 2010*, 2010.

[89] P. Jagadev and L. I. Giri, "Non-contact monitoring of human respiration using infrared thermography and machine learning," *Infrared Phys. Technol.*, vol. 104, Jan. 2020.

[90] H. Liu, J. Allen, D. Zheng, and F. Chen, "Recent development of respiratory rate measurement technologies," *Physiological Measurement*, vol. 40, no. 7. Institute of Physics Publishing, 02-Aug-2019.

[91] F. AL-Khalidi, R. Saatchi, H. Elphick, and D. Burke, "Tracing the Region of Interest in Thermal Human Face for Respiration Monitoring," *Int. J. Comput. Appl.*, vol. 119, no.

4, pp. 42–46, Jun. 2015.

[92] J. Fei and I. Pavlidis, “Thermistor at a distance: Unobtrusive measurement of breathing,” *IEEE Trans. Biomed. Eng.*, vol. 57, no. 4, pp. 988–998, Apr. 2010.

[93] G. F. Lewis, R. G. Gatto, and S. W. Porges, “A novel method for extracting respiration rate and relative tidal volume from infrared thermography,” *Psychophysiology*, vol. 48, no. 7, pp. 877–887, Jul. 2011.

[94] C. B. Pereira, X. Yu, M. Czaplik, R. Rossaint, V. Blazek, and S. Leonhardt, “Remote monitoring of breathing dynamics using infrared thermography,” *Biomed. Opt. Express*, vol. 6, no. 11, p. 4378, Nov. 2015.

[95] A. H. Alkali, R. Saatchi, H. Elphick, and D. Burke, “Facial tracking in thermal images for real-time noncontact respiration rate monitoring,” in *2013 European Modelling Symposium*, 2013, pp. 265–270.

[96] C. Barbosa Pereira, X. Yu, M. Czaplik, V. Blazek, B. Venema, and S. Leonhardt, “Estimation of breathing rate in thermal imaging videos: a pilot study on healthy human subjects,” *J. Clin. Monit. Comput.*, vol. 31, no. 6, pp. 1241–1254, Dec. 2017.

[97] R. Murthy, I. Pavlidis, and P. Tsiamyrtzis, “Touchless monitoring of breathing function,” *The 26th Annual International Conference of the IEEE Engineering in Medicine and Biology Society*, 2004, pp. 1196-1199.

[98] R. Murthy and I. Pavlidis, “Noncontact measurement of breathing function,” *IEEE Eng. Med. Biol. Mag.*, vol. 25, no. 3, pp. 57–67, 2006.

[99] S. L Bennett, R. Goubran, & F. Knoefel, “The Detection of Breathing Behavior Using Eulerian-Enhanced Thermal Video, ” *2015 37th Annual International Conference of the IEEE Engineering in Medicine and Biology Society (EMBC),* 2015, pp. 7474-7477.

[100] Kwasniewska, Ruminski, and Szankin, “Improving Accuracy of Contactless Respiratory Rate; Estimation by Enhancing Thermal Sequences with; Deep Neural Networks,” *Appl. Sci.*, vol. 9, no. 20, Oct. 2019.

[101] J. Shotton *et al.*, “Real-time human pose recognition in parts from single depth images,” *CVPR 2011,* 2011, pp. 1297-1304.

[102] J. Fei, I. Pavlidis, and J. Murthy, “Thermal vision for sleep apnea monitoring,” in *Lecture Notes in Computer Science (including subseries Lecture Notes in Artificial Intelligence and Lecture Notes in Bioinformatics)*, 2009.

[103] A. Seba, D. Istrate, T. Guettari, A. Ugon, A. Pinna, and P. Garda, “Thermal-Signature-Based Sleep Analysis Sensor,” *Informatics*, vol. 4, no. 4, p. 37, Oct. 2017.

[104] Z. Chen and Y. S. Wang, “Sleep monitoring using an infrared thermal array sensor,” 2019, p. 53.

[105] Z. Zhu, J. Fei, and I. Pavlidis, “Tracking human breath in infrared imaging,” *Fifth IEEE Symp. Bioinforma. Bioeng. (BIBE’05).,* vol. 2005, pp. 227–231, 2005.

[106] F. Q. Al-Khalidi, R. Saatchi, D. Burke, H. Elphick, and S. Tan, “Respiration rate

monitoring methods: A review," *Pediatric Pulmonology*. 2011.

[107] C. B. Pereira *et al.*, "Noncontact Monitoring of Respiratory Rate in Newborn Infants Using Thermal Imaging," *IEEE Trans. Biomed. Eng.*, vol. 66, no. 4, pp. 1105–1114, Apr. 2019.

[108] I. Lorato, T. Bakkes, S. Stuijk, M. Meftah, and G. de Haan, "Unobtrusive respiratory flow monitoring using a thermopile array: A feasibility study," *Appl. Sci.*, vol. 9, no. 12, Jun. 2019.

[109] J. Howse, *OpenCV Computer Vision with Python.* Packt Publishing, 2013.

[110] P. G. Kumbhar and S. N. Holambe, "A Review of Image Thresholding Techniques," *Int. J. Adv. Res. Comput. Sci. Softw. Eng.*, vol. 5, no. 6, 2015.

[111] P. Virtanen *et al.*, "SciPy 1.0: fundamental algorithms for scientific computing in Python," *Nat. Methods*, vol. 17, no. 3, 2020

[112] R. W. Schafer, "What is a savitzky-golay filter?," *IEEE Signal Process. Mag.*, vol. 28, no. 4, 2011.

[113] S. F. Allen *et al.*, "Exploration of potential objective and subjective daily indicators of sleep health in normal sleepers," *Nat. Sci. Sleep*, vol. 10, pp. 303–312, 2018.

[114] E. M. Rogers, A. Singhal, and M. M. Quinlan, "Diffusion of innovations," in *An Integrated Approach to Communication Theory and Research, Third Edition*, 2019.

[115] R. J. Hill, M. Fishbein, and I. Ajzen, "Belief, Attitude, Intention and Behavior: An Introduction to Theory and Research.," *Contemp. Sociol.*, vol. 6, no. 2, 1977.

[116] R. L. Thompson, C. A. Higgins, and J. M. Howell, "Influence of experience on personal computer utilization: Testing a conceptual model," *J. Manag. Inf. Syst.*, vol. 11, no. 1, 1994.

[117] V. Venkatesh, R. H. Smith, M. G. Morris, G. B. Davis, F. D. Davis, and S. M. Walton, "User acceptance of information technology: Toward a unified view," *MIS quarterly*, pp. 425-478, 2003.

[118] F. D. Davis, "Perceived usefulness, perceived ease of use, and user acceptance of information technology," *MIS Q. Manag. Inf. Syst.*, vol. 13, no. 3, 1989.

[119] R. L. Thompson, C. A. Higgins, and J. M. Howell, "Personal computing: Toward a conceptual model of utilization," *MIS Q. Manag. Inf. Syst.*, vol. 15, no. 1, 1991.

[120] G. C. Moore and I. Benbasat, "Development of an Instrument to Measure the Perceptions of Adopting an Information Technology Innovation Instrument development—Innovation diffusion—Information technology adoption—Research methodology," *Inf. Syst. Res.*, vol. 2, no. 3, 1991.

[121] P. J. Hu, P. Y. K. Chau, O. R. Liu Sheng, and K. Y. Tam, "Examining the Technology Acceptance Model Using Physician Acceptance of Telemedicine Technology," *J. Manag. Inf. Syst.*, vol. 16, no. 2, 1999.

[122] M. Y. Yi, J. D. Jackson, J. S. Park, and J. C. Probst, "Understanding information

technology acceptance by individual professionals: Toward an integrative view," *Inf. Manag.*, vol. 43, no. 3, 2006.

[123] A. Bhattacherjee and N. Hikmet, "Physicians' resistance toward healthcare information technology: A theoretical model and empirical test," *Eur. J. Inf. Syst.*, vol. 16, no. 6, 2007.

[124] T. T. Moores, "Towards an integrated model of IT acceptance in healthcare," *Decis. Support Syst.*, vol. 53, no. 3, 2012.

[125] S. Y. Hung, Y. C. Ku, and J. C. Chien, "Understanding physicians' acceptance of the Medline system for practicing evidence-based medicine: A decomposed TPB model," *Int. J. Med. Inform.*, vol. 81, no. 2, 2012.

[126] H. Liang, Y. Xue, W. Ke, and K. K. Wei, "Understanding the influence of team climate on it use," *J. Assoc. Inf. Syst.*, vol. 11, no. 8, 2010.